NTNU

Norwegian University of
Science and Technology

Fundamental mechanisms of density wave oscillations and the effect of subcooling

Dag Strømsvåg

Master of Science in Energy and Environment
Submission date: February 2011
Supervisor: Maria Fernandino, EPT
Co-supervisor: Leonardo Ruspini, EPT

Norwegian University of Science and Technology
Department of Energy and Process Engineering

Problem Description

The study of the dynamic behaviour of a thermal system operating in forced convection flow boiling is important for the prediction and understanding of the local and global stability phenomena. Two phase flow instabilities are undesirable as they can result in mechanical vibrations and system control problems, affect normal operation, restrict operating parameters and influence system safety. Several types of instabilities induced by boiling two phase flows are of relevance for the design and operation of industrial systems. The proper characterisation of the instabilities and the condition for its occurrence can determine optimal and safe operation of the involved systems.
The most accepted explanation for the occurrence of the dynamic type of instabilities called density wave oscillations (DWO) involves interactions and delayed feedbacks between the inertia of flow and compressibility of the two phase mixture. The characteristic periods of these oscillations are associated with the time required for a fluid particle to travel through the entire loop. Therefore the frequencies depend on the circuit geometry but it is normal to find DWO with frequencies between 1 and 10 Hz.
The main goal of this work will be to perform a theoretical analysis of density wave oscillations. The focused will be on the characterisation of the DWO, parameter analysis of the main effects in terms of the fluid properties, system geometry, etc.

The following tasks should be considered in the project work:

1. Review the state of the art of the characterisation of DWO.

2. Using an existing model for DWO, verify and validate the model against available information.

3. Perform a parametric analysis for identifying the effect of fluids and geometry.

4. Review the occurrence of DWO in different industries and the methodology used for limiting the operational region of the process.

Assignment given: 15. September 2010
Supervisor: Maria Fernandino, EPT

Abstract

Boiling two-phase flow is found in many industrial applications such as boiling water reactors, two-phase flow heat exchangers and refrigeration systems. The physics of two-phase gas-liquid flow may lead to undesirable system instabilities, and in the literature density wave oscillations (DWO) is reported to be the most commonly observed instability phenomenon. However, the literature also provides two opposing views on what the fundamental mechanism of DWO is. The so-called classical description of DWO focuses on the variation in mixture density as the governing mechanism, and the oscillation period will consequently be about one to two times the channel residence time. The findings presented in Rizwan-Uddin [1994] show that it is the variation in mixture velocity that has the dominating effect, and the oscillation period was reported to be closer to four times the channel residence time. Ambrosini et al. [2000] united the two opposing views by stating that the governing mechanism depends on the level of system subcooling. The classical description of DWO is based on a lower level of subcooling, while Rizwan-Uddin [1994] considered higher subcooling. Here, the fundamental mechanisms of DWO and the effect of system subcooling is investigated further by performing a numerical analysis using a one dimensional homogenous equilibrium flow model. The modeled system consists of a horizontal uniformly heated boiling channel with an inlet- and exit restriction. The system is exposed to constant externally imposed pressure drop. The effect of system subcooling is investigated by comparing the self-sustained periodic oscillations which make out the modeled stability threshold. The flow model is validated by observing the above mentioned effects of subcooling on DWO. Further, it is found that the change from a density dominated exit restriction towards a velocity dominated exit restriction is a smooth transition for increased subcooling. The amplitude of the variations in exit mixture velocity increases continuously with subcooling, and due to the squared relationship between the exit restriction pressure drop and the exit mixture velocity, velocity becomes the governing mechanism at high subcooling. The modeled stability threshold approaches a straight line at high subcooling. This line represents operating conditions which have the same mean boiling boundary location. However, the amplitude of the variations about this mean limit grows exponentially at high subcooling. The oscillation period of the observed DWO grows continuously with higher subcooling, and the period increases exponentially at high subcooling. In contrast, the mean boiling channel residence time approaches an upper mean limit at high subcooling. It is postulated that it is the transition towards a more mixture velocity dominated system that causes the oscillation period to evolve as it does with respect to the level of subcooling.

Contents

Nomenclature

Symbols

Symbol	Description	Unit
A	Cross-sectional area of boiling channel	[m^2]
D	Diameter of boiling channel	[m]
f	Friction factor	[-]
G	Mass flux	[kg/m^2s]
h	Enthalpy	[J/kg]
j	Superficial velocity	[m/s]
K	Restriction pressure drop coefficient	[-]
L	Length of boiling channel	[m]
p	Static pressure	[Pa]
Q	Volume flow	[m^3/s]
q	Power	[W]
S	Slip ratio	[-]
T	Temperature	[K]
t	Time	[s]
u	Velocity	[m/s]
W	Mass flow	[kg/s]
x	Vapor quality	[-]
z	Distance from boiling channel inlet	[m]

Greek Symbols

Symbol	Description	Unit
α	Void fraction	[-]
μ	Dynamic viscosity	[kg/ms]
ρ	Density	[kg/m^3]
θ	Angle	[rad]
τ	System restriction coefficient	[-]

Miscellaneous

Symbol	Description	Unit
Δp_{ext}	Externally imposed pressure drop	[Pa]
Δp_e	Exit restriction pressure drop	[Pa]
Δp_i	Inlet restriction pressure drop	[Pa]
f_{go}	Friction factor with saturated gas only	[-]
f_{lo}	Friction factor with saturated liquid only	[-]
h_{lg}	Latent heat of evaporation	[J/kg]
λ_b	Boiling boundary location	[m]
N_{pch}	Equilibrium phase-change number	[-]
N_{sub}	Subcooling number	[-]
q'	Added heat per unit length	[W/m]
Re_D	Reynolds number of circular channel	[-]
T_sat	Saturation temperature	[K]
u_s	Slip velocity	[m/s]
V_{gj}	Drift velocity of gas phase	[m/s]
V_{lj}	Drift velocity of liquid phase	[m/s]

Subscripts

Symbol	Description
e	Boiling channel exit
E	Exit pressure reservoir
g	Gas phase
i	Boiling channel inlet
I	Inlet pressure reservoir
l	Liquid phase
m	Homogenous mixture
p	Oscillation period
r	Residence time
$1p$	Single-phase region
$2p$	Two-phase region

Superscripts

Symbol	Description
max	Maximum value

1 Introduction

1.1 Background and Motivation

Boiling two-phase flow is found in many industrial applications such as boiling water reactors, two-phase flow heat exchangers, refrigeration systems and several chemical process devices [Kakac and Cao, 2009]. Utilizing a boiling fluid in heat exchangers is beneficial because it gives a high heat transfer rate at reasonable temperature differences [Yuncu et al., 1991]. On the other hand, the physics of two-phase gas-liquid flow may lead to undesirable system instabilities. Oscillations in pressure, mass flow and temperature can cause mechanical vibrations, high pressure and in some cases even rupture the heat transfer surface [Dogan et al., 1983]. Due to the possible fatal consequence of such instabilities, there has been extensive research devoted to boiling two-phase flow. Excellent reviews on two-phase flow instabilities are presented in Boure et al. [1973] and Kakac and Bon [2008].

Density wave oscillations (DWO) is in the literature reported as the most common type of two-phase flow instabilities [Ding et al., 1995], and is considered to be at the basis of the most frequently observed instabilities in boiling channel systems [Ambrosini et al., 2000]. DWO is a result of multiple regenerative feedbacks between the flow rate, vapor generation and pressure [Boure et al., 1973]. For certain system conditions these oscillations may become self-sustained with constant a period and amplitude. This low frequency oscillatory phenomenon has its name from the fact that the oscillation period is in the order of the time it takes for a resulting density wave to propagate through the system [Ding et al., 1995]. Traditionally, it is believed that these oscillations have a period that is about one to two times the boiling channel residence time, and that the variation in mixture density plays an important part in the resulting oscillations [Kakac and Bon, 2008]. Rizwan-Uddin [1994] raised criticism towards this classical description. Based on a numerical investigation he showed that for the parameter space considered the emphasis should be put on variations in mixture velocity rather than the variations in mixture density. Rizwan-Uddin [1994] presented results where the modeled oscillations had a period closer to four times the channel residence time. The criticism of Rizwan-Uddin [1994] acts as the starting point for Ambrosini et al. [2000], who adds additional information for discussing the mechanisms of DWO. The findings of Ambrosini et al. [2000] state evidence that support both the classical description of DWO and the contradicting view of Rizwan-Uddin [1994]. The opposing views are according to Ambrosini et al. [2000] a result of the difference in the applied level of subcooling. The classical description is based on a low system subcooling, while the description of Rizwan-Uddin [1994] is considering a higher level. Ambrosini et al. [2000] concludes that the relative weight of either mechanism (mixture density and velocity) is different depending on the level of subcooling, and that one should avoid focusing on a single effect.

In order to avoid the unwanted effects of unstable oscillations occurring in boiling two-phase flow systems, it is important that the system designer and the operator is able to predict the onset of instability and operate the system within a safe margin of the so-called marginal stability threshold. Pioneer work in the search

for understanding the onset of instability was performed by Ishii and Zuber [1970], and led to the development of a stability map based on two non-dimensional scaling parameters, namely the phase-change number N_{pch} and the subcooling number N_{sub}. These parameters are defined for the boiling system at hand, and through theoretical and experimental research one has developed stability thresholds aiding in the safe operation of boiling two-phase flow systems.

1.2 Objective

The main objective of this thesis is to perform a numerical analysis of density wave oscillations. The focus will be put on the fundamental mechanisms of DWO and the effect of subcooling. A second objective is to verify and validate the applied two-phase flow model against available information.

1.3 Scope of Work

Density wave oscillations will be investigated in a horizontal single boiling channel with inlet and exit restrictions. The system is exposed to a constant externally imposed pressure drop. The boiling channel is subjected to constant uniform heat flux with water at low pressure as the working fluid. An already developed numerical model assuming one dimensional, thermo-dynamic equilibrium flow is used for studying the dynamic behavior of the system. The utilized flow model is based on that presented in Ruspini et al. [2009] and Ruspini et al. [2010].

2 Fundamentals of Two-phase Flow

Two-phase flow is a term covering the interaction between two phases (gas, liquid or solid) where the interface between them is influenced by their motion [Butterworth and Hewitt, 1979]. This paper is concerned with boiling two-phase flow, where the working fluid may experience a phase-change as it progress through the heated system. Hence, the fluid ca be in a state of gas, liquid or a combination of both. This section will introduce basic theory concerning gas-liquid two-phase flow.

2.1 Fundamental Definitions

The properties of the two phases in gas-liquid flow are distinguished by the subscripts g and l, respectively.

2.1.1 Vapor Quality

The vapor quality x is a convenient measure of how much of the total mass flow in a system is occupied by the gas phase, and is defined as:

$$x = \frac{W_g}{W} \tag{1}$$

where W_g [kg/s] is the mass flow rate of the gas phase and W [kg/s] is the total mass flow rate.

In boiling or condensing applications the amount of gas (and liquid) in the system changes as the fluid is heated or cooled. The so-called thermodynamic equilibrium quality assumes that both phases are saturated at the same temperature T_{sat} corresponding to their common pressure. Equation 2 shows how the thermodynamic equilibrium quality is determined:

$$x = \frac{h_m(z) - h_l}{h_{lg}} \tag{2}$$

where h_l [J/kg] is the saturated liquid enthalpy, h_{lg} [J/kg] is the latent heat of evaporation, and $h_m(z)$ [J/kg] is the average two-phase mixture enthalpy at the cross-section a distance z [m] from the inlet. The average mixture enthalpy can be calculated as shown in equation 3:

$$h_m(z) = h_{m,i} + \frac{1}{W}\int_0^z q'(z)dz \tag{3}$$

where $h_{m,i}$ [J/kg] is the mixture enthalpy at the inlet of the channel, and $q'(z)$ [W/m] is the heat added per unit length of the channel. Both definitions of the vapor quality (equation 1 and 2) coincide if the two phases are at thermodynamic equilibrium.

2.1.2 Void Fraction

In gas-liquid flow the void fraction α represents the volumetric concentration of the gas present in the system. As it determines mean velocities of the liquid and gas, it represents a fundamental parameter in the calculation of pressure drop, flow pattern transitions and heat transfer coefficients. The void fraction is defined as:

$$\alpha = \frac{A_g}{A} \tag{4}$$

where A_g [m^2] is the cross-sectional area occupied by the gas phase and A [m^2] is the total area of the channel cross-section. Figure 1 illustrates the above.

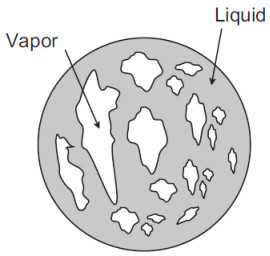

Figure 1: Cross-sectional void fraction (α) [Quiben, 2005].

2.1.3 Velocities

True average velocity This is the velocity that each of the two phases actually travel with. Equation 5 and 6 give the true average velocity for the gas and liquid phase, respectively,

$$u_g = \frac{Q_g}{A_g} = \frac{Q_g}{\alpha A} \tag{5}$$

$$u_l = \frac{Q_l}{A_l} = \frac{Q_l}{\alpha A} \tag{6}$$

where Q_g [m^3/s] and Q_l [m^3/s] are the volumetric flow rates of the respective phases.

Mass Flux The mass flux G [kg/m^2s] is defined as the total mass flow rate W [kg/s] divided by the total cross-sectional area A [m^2]:

$$G = \frac{W}{A} \tag{7}$$

The mass fluxes of the gas and liquid phase are defined respectively as:

$$G_g = Gx \tag{8}$$
$$G_l = G(1-x) \tag{9}$$

Superficial velocity If the two phases would be flowing alone in the channel they would experience what is known as their superficial velocity. The superficial velocity of the respective gas and liquid phases are defined as:

$$j_g = \frac{Q_g}{A} = \frac{Gx}{\rho_g} = u_g\alpha \tag{10}$$
$$j_l = \frac{Q_l}{A} = \frac{G(1-x)}{\rho_l} = u_l(1-\alpha) \tag{11}$$

The total superficial velocity is given as:

$$j = j_g + j_l \tag{12}$$

Drift velocities and Drift flux It is sometimes convenient to consider a relative velocity of each phase. The drift velocity shows the relative motion of the gas and liquid phase compared to a surface perpendicular to the direction of the flow. This surface moves with the total superficial velocity j given by equation 12. For the gas and liquid phase the drift velocity is respectively defined as:

$$V_{gj} = u_g - j \tag{13}$$
$$V_{lj} = u_l - j \tag{14}$$

The drift flux represents the volumetric flux relative to the above mentioned surface, and is for the gas and liquid phase respectively defined as:

$$j_{gj} = \alpha V_{gj} = \alpha(u_g - j) \tag{15}$$
$$j_{lj} = (1-\alpha)V_{lj} = (1-\alpha)(u_l - j) \tag{16}$$

Slip velocity The gas and liquid phase often flow with different velocities. The slip velocity u_S is defined as the difference between the true average velocity of the gas and liquid phase, respectively:

$$u_s = u_g - u_l \tag{17}$$

The slip ratio is given as:

$$S = \frac{u_g}{u_l} \tag{18}$$

2.2 Choosing a Two-phase Flow Model

Because of the unwanted instabilities found in boiling two-phase flow systems, mathematical modeling is needed to assist in the determination of safe operating regions. In the literature we find three common models used in the modeling of two-phase flows: 1) the homogeneous equilibrium model; 2) the drift flux model; and 3) the general two-fluid model. The latter is cumbrous to treat analytically [Rizwan-Uddin and Dorning, 1986], and it is therefore common to choose between either of the first two. The modeling of two-phase flow performed in this paper is based on the homogeneous equilibrium model (HEM). Hence, only the HEM model will be presented here. The reader is referred to Munkejord [2006] for information regarding the drift flux model and the two-fluid model.

2.2.1 Homogeneous Equilibrium Model

Homogeneous flow theory provides the simplest technique for analyzing two-phase flow, and the advantage lies in its simplicity. The gas-liquid mixture is regarded as a pseudo-fluid which allow us to treat it as any other single-phase fluid. All of the standard methods of fluid mechanics are therefore applicable. The pseudo-fluid properties are weighted averages, and are not necessarily the same as the properties of either phase. The required average properties are velocity, thermodynamic properties, and transport properties (e.g. viscosity). If we assume that the velocity and temperature of the individual phases are the same, we end up with a so-called *homogeneous equilibrium flow* [Wallis, 1969]. Even though these simplifications naturally lead to some deviation from the actual system dynamics, it is believed that the HEM model will provide very useful information regarding the gross behavior of the boiling channel system [Ambrosini et al., 2000].

As stated above, the assumption of regarding the two-phase mixture as a single-phase pseudo-fluid, allows us to utilize basic single-phase flow mechanics to study the flow. Equation 19, 20 and 21, as found in Wallis [1969], show the conservation equations for mass, momentum and energy, respectively:

$$\frac{\partial \rho_m}{\partial t} + \frac{\partial G}{\partial z} = 0 \tag{19}$$

$$\frac{\partial G}{\partial t} + \frac{\partial}{\partial z}\left(\frac{G^2}{\rho_m}\right) = -\frac{\partial p}{\partial z} - \rho g \cos\theta - \frac{f_m}{2D}\frac{G^2}{\rho_m} \tag{20}$$

$$\frac{\partial h_m}{\partial t} + \frac{G}{\rho_m}\frac{\partial h_m}{\partial z} = \frac{1}{\rho_m}\left[\frac{\partial p}{\partial t} + \frac{G}{\rho_m}\frac{\partial p}{\partial z}\right] + \frac{f_m}{2D}\frac{G^3}{\rho_m} + \frac{1}{A\rho_m}\frac{\partial q}{\partial z} \tag{21}$$

where ρ_m [kg/m^3] is the average mixture density, G [kg/m^{2}s] is the mass flux, and p [Pa] is the static pressure. The pipe has an inclination of θ [rad] to the vertical. For a horizontal pipe $\theta = \pi/2$. The heated pipe has a diameter D [m] and a cross-sectional area A [m^2]. h_m [J/kg] is the average mixture enthalpy. The pipe is heated with a total power of q [W]. The homogenous mixture friction factor f_m is the only empirical parameter in the above set of equations, and it is determined from correlations found in the literature (see section 2.2.2). The friction factor

found in equation 20 and 21 is known as Darcy's friction factor, which is related to the other well known friction factor of Fanning by $f_m = 4C_f$.

2.2.2 Frictional Pressure Drop Correlations

In order to determine the pressure drop due to friction, the friction factor f_m must be determined. In the case where the subscript m is not present, the flow is assumed to be single-phase liquid or gas. Since it is an empirical parameter, it can be found from correlations presented in the literature. In all viscous flows the primary controlling parameter is the dimensionless Reynolds number [White, 1991]. Consequently, the Reynolds number is important in friction factor correlations. For a circular pipe the Reynolds number is defined as:

$$\mathrm{Re}_D = \frac{GD}{\mu} \tag{22}$$

where μ [kg/ms] is the fluid dynamic viscosity. As the Reynolds number Re_D increases, the flow evolves from a smooth *laminar* state, through a transitional region, into a fluctuating *turbulent* regime. The boiling channel system considered in this paper will have single-phase liquid at the inlet, and possibly single-phase vapor at the outlet. In some region of the boiling channel, two-phase flow will occur. It is therefore important to choose a frictional pressure drop correlation accordingly.

Single-Phase Flow In single-phase flow, being either pure liquid or pure gas flow, several different friction factor correlations are found depending on the Reynolds number. In this paper, the following correlations are implemented for single-phase flow:

$$Re_D < 2000: \qquad f = \frac{64}{\mathrm{Re}_D} \tag{23}$$

$$2000 \leq Re_D < 4000: \qquad f = (\mathrm{Re}_D - 2000)\,\frac{\frac{0.316}{\mathrm{Re}_D^{0.25}} - \frac{64}{\mathrm{Re}_D}}{2000} + \frac{64}{\mathrm{Re}_D} \tag{24}$$

$$4000 \leq Re_D < 10^5: \qquad f = \frac{0.316}{\mathrm{Re}_D^{0.25}} \tag{25}$$

$$Re_D > 10^5: \qquad f = \frac{1}{\left(1.8\log\left(\frac{\mathrm{Re}_D}{6.9}\right)\right)^2} \tag{26}$$

where equation 23 is the well known correlation for laminar flow [White, 1991], and equation 24 represents the single-phase friction experienced in the transitional region White [1991]. Equation 25 is the Blasius equation for turbulent flow, and equation 26 is the Colebrook equation as found in White [1991].

Two-Phase Flow In order to determine the friction factor for two-phase flow, two-phase flow pressure drop correlations are used. Several different correlations

are available in the literature, but here only the correlation of Muller-Steinhagen and Heck [1986] will be presented, as it is the correlation implemented in this paper. The reader is referred to Quiben [2005] for a presentation of additional available correlations.

The Muller-Steinhagen and Heck [1986] correlation is an empirical interpolation between the frictional pressure drop for liquid-only flow and gas-only flow. The two-phase friction factor is correlated as:

$$f_m = F\left(1-x\right)^{\frac{1}{3}} + Bx^3 \tag{27}$$

where x is the thermo-dynamic mixture quality defined as in equation 2, and:

$$F = A + 2\left(B - A\right)x \tag{28}$$

$$A = f_{lo}\frac{\rho}{\rho_l} \tag{29}$$

$$B = f_{go}\frac{\rho}{\rho_g} \tag{30}$$

The subscripts lo and go denote the friction factor when the entire flow G is assumed to be saturated liquid and gas, respectively. Hence, the friction factors f_{lo} and f_{go} are calculated using the single-phase correlations given by equation 23 to 26, depending on the Reynolds number found using equation 22. The Muller-Steinhagen and Heck [1986] correlation is valid for $0 \leq x \leq 1$.

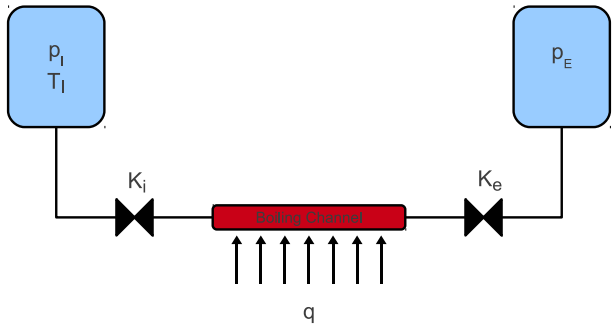

Figure 2: Schematic of a simple boiling channel system.

3 Density Wave Oscillations

Flow instabilities are undesirable in boiling channel systems because sustained oscillations may cause mechanical vibration and system control problems. In some cases, the oscillations may even rupture the heat transfer surface due to boiling crisis (dry-out, burnout) [Boure et al., 1973]. A boiling channel system forms a complex thermal-hydrodynamic system with dynamic characteristics [Belblidia and Bratianu, 1979], and the delayed propagation of disturbances and the resulting feedback lead to *dynamic instabilities* [Kakac and Bon, 2008]. Density wave oscillations (DWO) is a part of this group of instabilities, and is reported to be the most commonly observed two-phase flow instability [Boure et al., 1973, Kakac and Bon, 2008, Ding et al., 1995, Ambrosini et al., 2000].

3.1 Mechanisms of DWO

Consider the system shown in figure 2 which is currently operating at steady state. The system is exposed to a constant externally imposed pressure drop given by the inlet- and exit pressure reservoir p_I and p_E, respectively. Two flow restrictions are placed at the inlet and exit of the boiling channel with respective restriction coefficients K_i and K_e. The boiling channel is heated with constant uniform heat q. For the sake of simplicity we assume that the system pressure drop is concentrated at the inlet and exit restrictions.

Density wave oscillations is triggered by a perturbation in one of the system's boundary conditions. Here, we assume that at time $t = 0$ the exit restriction experiences a small drop in its pressure drop Δp_e. Since the total system pressure drop is constant, a drop in Δp_e will lead to an equal opposite sign change in the inlet restriction pressure drop Δp_i. The now larger Δp_i yields a lower channel inlet pressure p_i, due to the constant inlet reservoir pressure p_I. The boiling channel

inlet velocity u_i will consequently increase because of the relation $u_i \propto \sqrt{p_I - p_i}$. All this happens at the speed of the sound in the fluid, which is regarded as instantaneous. A higher inlet velocity with respect to the initial steady state value, will cause a wave of higher density fluid to propagate through the channel. Once at the exit some time later, the denser fluid will cause an increase in Δp_e, which is followed by an instantaneous decrease in Δp_i. The inlet velocity is consequently decreased, and a wave of lower density fluid will move towards the exit. As it reaches the exit restriction the pressure drop there decreases again. The cycle is complete, and the same procedure is repeated. For certain combinations of system dimensions, operating conditions, and boundary conditions, the inlet perturbations can acquire an appropriate exit pressure fluctuation which leads to self-sustained periodic oscillations.

A similar reasoning as to the above can be found in the literature, and is regarded as the *classical description* of DWO [Kakac and Bon, 2008, Belblidia and Bratianu, 1979, Ambrosini et al., 2000, Rizwan-Uddin, 1994]. It is evident from this postulated behavior that the oscillations will have a period equal to about twice the boiling channel residence time, which is the time needed for a wave of both higher and lower density to travel through the system. The exit pressure drop oscillations, which is fed back to the inlet, will vary close to in-phase with the local density perturbations [Ambrosini et al., 2000]. The traveling density wave is by the classical description given a fundamental role in explaining the nature of the oscillations [Rizwan-Uddin, 1994]. It is also believed that in order to experience self-sustained oscillations, the inlet perturbation must acquire a 180°out-of-phase pressure fluctuation at the exit, which is immediately transmitted to the inlet flow rate [Boure et al., 1973].

In Rizwan-Uddin [1994] criticism was raised towards the classical description of DWO on the basis of the emphasis it gives the role of density waves. By numerically investigating a boiling channel system similar to that shown in figure 2, though with a vertical up-flow channel, Rizwan-Uddin [1994] discovered that in the parameter space considered, density waves could not be characterized as a fundamental mechanism. Rizwan-Uddin [1994] suggested that the emphasis should be put on variations in mixture velocity rather than mixture density. His first argument was that the exit restriction pressure drop, instead of varying in-phase with exit density, varied more strongly with the behavior of the exit velocity. In addition to this, Rizwan-Uddin [1994] discovered that a strong density wave, represented by time delayed oscillations in mixture density downstream of the inlet, was not present during self-sustained oscillations. The mixture density varied almost simultaneously through out the two-phase region. A third important finding was also presented, where the period of the oscillations was close to four times the average channel residence time, rather than two as it is historically believed to be. This evidence clearly supports his conclusion that mixture density variations are not of paramount importance for the occurrence of DWO.

The above summarized criticism of Rizwan-Uddin [1994] was the starting point for yet another numerical research performed by Ambrosini et al. [2000]. The latter investigation set out to provide additional information for discussing the

fundamental mechanisms of DWO, and performed an analysis similar to that of Rizwan-Uddin [1994]. Ambrosini et al. [2000] stressed that the limitation of the homogenous equilibrium model (HEM), which was the two-phase flow model applied in the both investigations, should be duly considered to avoid extending the validity of the obtained results beyond reasonable limits. On the other hand, he states that the HEM model has been proven to provide useful information regarding the behavior of a boiling channel under unstable conditions. Ambrosini et al. [2000] found that for operating conditions yielding high subcooling (inlet temperature significantly less than the saturation temperature), it was possible to confirm the picture presented by Rizwan-Uddin [1994]. The period of the oscillations were in fact considerably larger than two times the boiling channel residence time, and the exit mixture density did not vary in-phase with exit pressure drop oscillations. Hence, the phenomena of DWO at high subcooling rely more on exit velocity fluctuations rather than variation in mixture density. Nevertheless, when considering oscillations at low subcooling, it was found that the modeled system did behave in great similarity with what is proposed by the classical description. In summary, as Ambrosini et al. [2000] partly expected, the obtained results show that fluctuations in mixture density and velocity superimpose and interact during DWO. He suggests that a comprehensive description of the DWO phenomena should avoid focusing on a single effect. The relative weight of either mechanism is different depending on the parameter space considered.

3.2 Stability of Boiling Two-Phase Flow Systems

Two-phase flow instabilities may have detrimental effects on a boiling system. The system designer has an important task in predicting the threshold of instability so that it can be designed around, or compensated for [Boure et al., 1973]. A great tool in the effort towards predicting such a stability threshold, and in this case with regards to DWO, is the two-dimensional stability map introduced by Ishii and Zuber [1970]. The characteristic equations of the two-phase flow model presented in Ishii and Zuber [1970] revealed two non-dimensional scaling parameters which proved to show a relation applicable in determining flow stability. These parameters, being the phase-change number N_{pch} and the subcooling number N_{sub}, are used as the x- and y-axis of the stability map, respectively. In this section we will first present these parameters, before reviewing the basic features of the stability map. The stability effect of various system parameters will also be presented.

3.2.1 The Equilibrium Phase-change Number

The phase-change number presented here is based on the assumption of thermal equilibrium, which differs from the non-equilibrium assumption in how one determines the location of the boiling boundary. According to the thermal equilibrium model, no significant vapor generation starts until the liquid bulk temperature reaches that of the saturation value. For the non-equilibrium assumption, the boiling boundary location, λ_b, is where a chosen significant amount of vapor generation starts. Further details regarding the latter is given in Saha et al. [1976]. The equi-

librium phase-change number is here defined as in equation 31 [Guido et al., 1991]. It can also be derived from the more extensive presentation given in Ishii and Zuber [1970] and Saha et al. [1976]. The phase-change number is calculated for channel inlet properties:

$$N_{pch} = \frac{q}{G_i A} \frac{\frac{1}{\rho_l} - \frac{1}{\rho_g}}{\frac{1}{\rho_l}(h_l - h_g)} \tag{31}$$

where q [W] is the constant uniform power added to the boiling channel, G_i [kg/m^{2}s] is the inlet mass flux, and A [m^2] is the cross-sectional area of the channel. The subscripts l and g denote saturated properties at the inlet of the liquid and gas phase, respectively. N_{pch} scales the rate of phase-change due to heat addition [Saha et al., 1976], and the equality of N_{pch} for two different systems ensures that the phase change has progressed equally in both, and thereby allowing us to compare them [Ishii and Zuber, 1970].

3.2.2 The Subcooling Number

The subcooling number N_{sub} scales the inlet subcooling and can be viewed as the dimensionless residence time of a fluid particle in the single-phase region [Saha et al., 1976]. Again, the definition used here is as found in Guido et al. [1991]. The subcooling number is defined as:

$$N_{sub} = (h_l - h_{m,i}) \frac{\frac{1}{\rho_l} - \frac{1}{\rho_g}}{\frac{1}{\rho_l}(h_l - h_g)} \tag{32}$$

where $h_{m,i}$ [J/kg] is the mixture enthalpy at the inlet of the boiling channel.

3.2.3 Stability Map

Ishii and Zuber [1970] proposed a two-dimensional stability map where the earlier defined scaling parameters N_{pch} and N_{sub} are used as the x- and y-axis, respectively. In figure 3, three theoretically determined stability thresholds, obtained from the same experimental system, are shown [Saha et al., 1976]. The given thresholds are the equilibrium theory of Ishii and Zuber [1970], the non-equilibrium theory of Saha and Zuber [1978], and the simplified stability criteria of Ishii [1971]. The latter is an explicit expression (see equation 33) derived from a thermal equilibrium flow model.

System operating conditions situated to the left of the solid blue line ($x_e = 0$) indicate a boiling channel exit quality less than zero, and consequently the boiling channel system operates solely with *single-phase liquid*. The region to the right of the dotted blue line ($x_e = 1$) yields superheated vapor at the channel exit. In the *stable region*, which is the region separated between the zero exit quality line and the various stability thresholds, the boiling channel system is able to damp perturbations and return itself back to the initial stable operating condition. According to Belblidia and Bratianu [1979], this is due to the dominance of the damping effect caused by friction. Operating conditions situated on a stability threshold will in

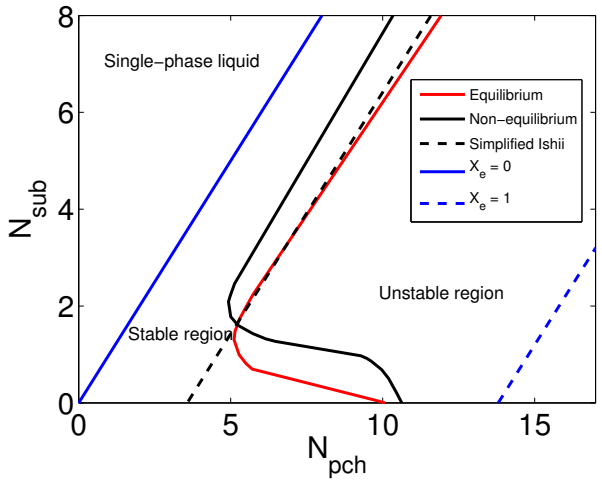

Figure 3: Stability map based on data presented in Saha et al. [1976]

theory produce self-sustained periodic oscillations. Such an oscillatory behavior is also referred to as marginally stable oscillations. Operating the boiling two-phase flow system in the region to the right of a stability thresholds will according to such a map, when experiencing a perturbation, produce diverging oscillations, which in time will grow out of proportions. In the latter *unstable region*, it is the driving effects of acceleration and gravity in the two-phase region that are predominant and cause the diverging flow behavior [Belblidia and Bratianu, 1979]. In figure 4 the oscillatory behavior of a converging and diverging flow is shown, representing the behavior of the stable- and unstable region, respectively. As stated earlier, the far right dotted blue line indicate that the boiling channel is experiencing single-phase vapor flow at the exit. Even though the effect of system operating pressure is absorbed by N_{pch} and N_{sub}, the operating pressure reveals itself in the location of the $x_e = 1$ line. At higher or lower operating pressures, the latter line is shifted towards the left or right, respectively [Saha et al., 1976].

The simplified stability criteria of Ishii [1971], based on a thermal equilibrium flow model, is expressed as:

$$N_{pch} = N_{sub} + \frac{2[K_i + \frac{f_m}{2D_h^*} + K_e]}{1 + \frac{1}{2}[\frac{f_m}{2D_h^*} + 2K_e]} \tag{33}$$

where K_i and K_e are the inlet and exit restriction pressure drop coefficient, respectively. In the case of equation 33, f_m is an assumed constant two-phase flow friction factor. $D_h^* = D_h/L$ where D_h [m] is the channel hydraulic diameter and L [m] is the boiling channel length. The simplified criteria of Ishii [1971] is believed to be valid for $N_{sub} > \pi$ [Saha et al., 1976].

Guido et al. [1991] studied DWO in parallel boiling channels. The research led

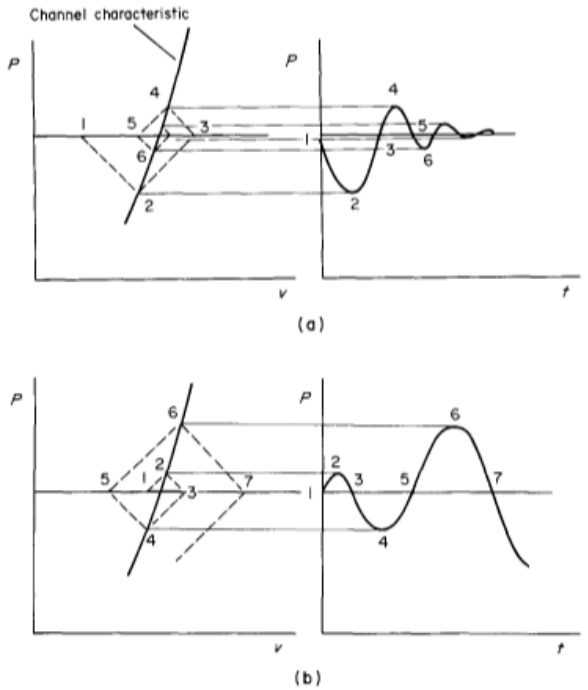

Figure 4: Oscillatory behavior: (a) convergent oscillation (b) divergent oscillation [Belblidia and Bratianu, 1979]

to an explicit expression for the marginal stability threshold of a single boiling channel derived directly from the applied flow model. The numerical study in Guido et al. [1991] is based on a homogenous equilibrium two-phase flow model assuming thermal equilibrium, constant externally imposed system pressure drop, and concentrated pressure drop at the channel inlet and outlet. The explicit expression is given as:

$$N_{pch} = N_{sub} + \frac{\tau}{2}\left(1 + \frac{2}{N_{sub}}\right) - \frac{5}{2}\left\{\left[\frac{\tau}{2}\left(1 + \frac{2}{N_{sub}}\right) - \frac{5}{2}\right]^2 + \tau\right\}^{1/2} \tag{34}$$

where τ is the system restriction coefficient given as:

$$\tau = \frac{2(K_i + K_e)}{K_e + 1} \tag{35}$$

As expressed in equation 34, the relation between N_{pch} and N_{sub} is given by the system restriction coefficient τ shown in equation 35. In figure 5 the stability threshold of Guido et al. [1991] is shown together with the theoretical thresholds of Saha et al. [1976]. In figure 5 the inlet and exit restrictions coefficients are $K_i = 5.7$ and $K_e = 4.06$, respectively. The values of K_i and K_e are inserted into equation 35 and 34, thereby obtaining the threshold of Guido et al. [1991]. All of the thresholds shown in figure 5 are found for the K-values given above.

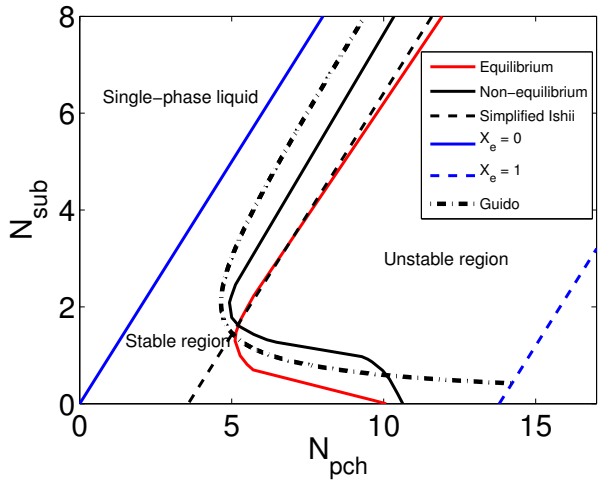

Figure 5: Stability map based on data presented in Saha et al. [1976] and results from Guido et al. [1991]

3.2.4 Stability Effect of Operational Parameters

Changing the operating parameters of a boiling channel system will affect the system behavior, and because density wave oscillations is the most commonly observed two-phase flow instability, the parametric effect on the observed oscillations have been studied by several investigators [Boure et al., 1973, Belblidia and Bratianu, 1979]. In this section, we will review what is presented in Belblidia and Bratianu [1979], but similar reviews can also be found in Boure et al. [1973] and Kakac and Bon [2008]. The review of parametric analysis presented in Belblidia and Bratianu [1979] assumes that the effects of a change can be separated and varied in turn while the remaining stay constant.

Effect of inlet velocity Increasing the inlet velocity of a boiling channel system has a stabilizing effect, regardless of the system subcooling or boiling channel power input. This can be best visualized by picturing a system operating condition located on the marginal stability thresholds given in figure 3. By increasing the inlet velocity, we increase the inlet mass flux, and the phase-change number N_{pch} given in equation 31 will consequently decrease. Thus, the operating point is moved into the stable operating region.

Effect of power input An increase of the boiling channel power input will destabilize the system. This effect can be explained in the same manner as above, but now with an increase of N_{pch}, moving the operating point into the unstable region.

Effect of subcooling The effect of changing the subcooling of a boiling two-phase flow system depends on the current level of subcooling. If operating at intermediate or high subcooling, an increase in subcooling would stabilize the system. At low subcooling the opposite effect is observed.

Effect of system pressure The increase of system pressure at a given power input will have a stabilizing effect on the system similar to that experienced when decreasing the power input, or increasing the flow rate as stated above. An increased system pressure reduces the void fraction and therefore the two-phase friction and momentum pressure drop. The void-response to perturbations are thereby reduced [Boure et al., 1973].

Effect of restrictions The parametric effect of inlet and exit restrictions has been investigated by numerous investigators (see Belblidia and Bratianu [1979]). An increase of the inlet restriction coefficient will add to the single-phase pressure drop, and hence increase the damping effect. The opposite is experienced when increasing the exit restriction coefficient, which adds to the two-phase pressure drop and increases the time delayed pressure drop. The effect of changing the inlet and exit restrictions can be pictured by plotting the stability threshold of Guido et al. [1991] for different values of K_i and K_e. In figure 6 we see that the area of

the stable- and unstable region is changed as the restriction coefficients are varied. The observed change is according to the above.

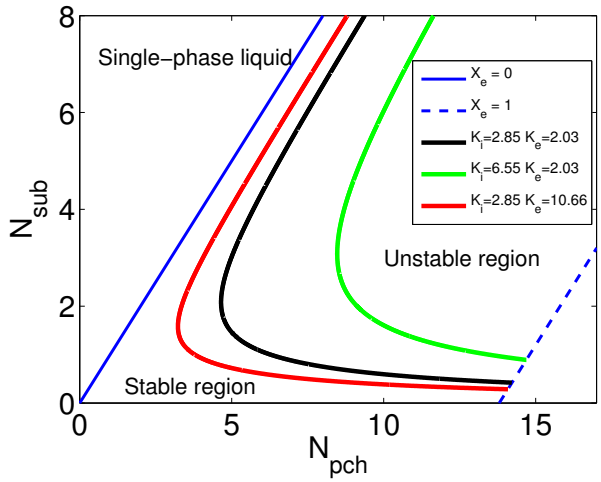

Figure 6: Stability thresholds of Guido et al. [1991] for different values of inlet- and exit restrictions.

3.3 DWO in Boiling Water Reactors

The delayed feedback phenomenon seen in boiling channel systems, commonly represented by the density wave, is the fundamental mechanism for flow instabilities in a boiling water reactor (BWR). Analyses of, and operating experiences from BWRs have shown that such systems are most likely to be susceptible to two kinds of instabilities; 1) channel flow instabilities, and 2) coupled neutronic-thermohydraulic instability. The former is what we have previously defined as DWO, which in BWRs can be observed in either a single channel or in parallel channels found in the reactor coolant core. Coupled neutronic-thermohydraulic instability is the most dominant of the two, and is consequently the most relevant for safe operation. The objective of the current section is merely to the state presence and the effect of DWO in BWR. Hence, only a minimum of the system's working principle will be presented. As the reader probably realize, to fully understand the highly complicated dynamic system of a BWR is beyond the scope of this work. Nevertheless, the author will try to present this review to the best of his ability. This review is a short summary of March-Leuba [1992] and March-Leuba and Rey [1993], and the reader is referred to these investigations for further details.

3.3.1 Channel Flow Instabilities

As already mentioned, channel flow instability is best described as what we defined earlier as DWO (see section 3.1). Even though the occurrence of this instability

type in BWRs is dominated by the coupled neutronic-thermohydraulic instability type (see section 3.3.2), it has however been observed in commercial BWRs. In the mid 1960s, one of the core's heated channels in the Garigliano reactor in Italy was running a special test when a flow meter at the exit of the respective channel failed in locked position. Consequently, the exit pressure drop increased significantly and the boiling channel became unstable. This is in accordance to what we reviewed in section 3.2.4 regarding the stability effect of a change in the exit restriction coefficient. In BWR this phenomenon might lead to fuel clad failure in the unstable channel, meaning that the fuel surface is damaged by preventing surface re-wetting due to by boiling crisis. A large BWR might have up to 800 channels, and a single channel instability might go unnoticed since the Average Power Range Monitor (APRM) is not able to detect the local instability. The reactor does only take protective action based on the APRM. The instability will often be seen by the Local Power Range Monitor (LPRM), but an action based on the LPRM must be done manually by the operator.

3.3.2 Coupled Neutronic-Thermohydraulic Instability

The power generation in BWRs is directly related to the fuel neutron flux, which is strongly related to the average void fraction in the core channels through what is know as the reactivity feedback. As opposed to the channel flow instability where the fuel power generation is stable, the coupled neutronic-thermohydraulic instability also involves oscillations in the generated heat. The currently reviewed instability is divided into two commonly recognized oscillation modes, being a) core-wide or in-phase mode, and b) the regional or out-of-phase mode. In the former, the power generation in the core and the core flow itself oscillate in-phase for all channels. In the out-of-phase mode, the power generation of half of the core oscillate out-of-phase with respect to the other. The same is true for the core flow. The power generation is monitored both globally and locally with the Average Power Range Monitor (APRM) and the Local Power Range Monitor (LPRM), respectively. The APRM is only able to disclose in-phase mode oscillations since the out-of-phase mode oscillations will average each other out. This was the case for the Ringhals BWR, where the measured neutron flux was as shown in figure 7. As you can see the oscillations of LPRM in the respective regions give a close to steady reading in the APRM. The out-of-phase mode is very dangerous to systems that does not have an automated protection against this type of instability mode. For the Ringhals incident, the shut-down was performed manually by the operator. In figure 8, observed in-phase mode oscillations are shown for the LaSalle reactor dating back to March 1988. These readings resulted in a automatic scram based on the APRM.

3.3.3 Sensitivity to Physical Parameters

The reactor stability is affected by most parameters. In the following some of the ways of affecting the core-wide instability mode will be presented, as they are given in March-Leuba [1992].

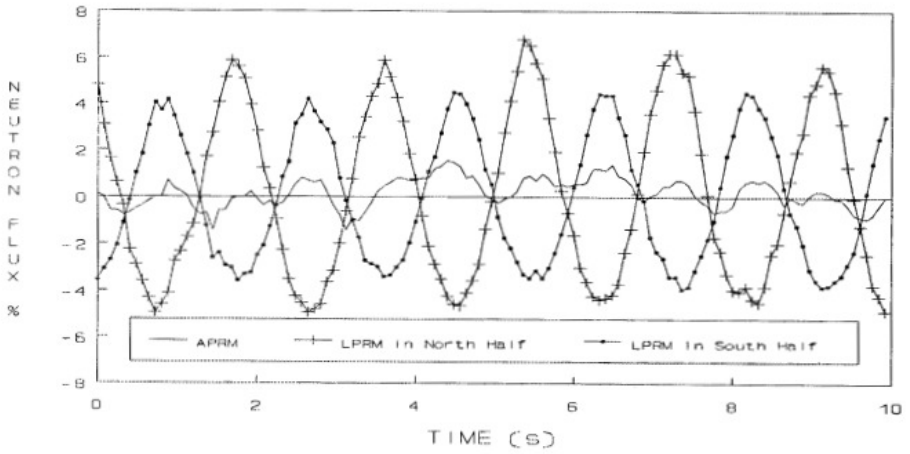

Figure 7: Average power range signal response to an out-of-phase instability [March-Leuba, 1992].

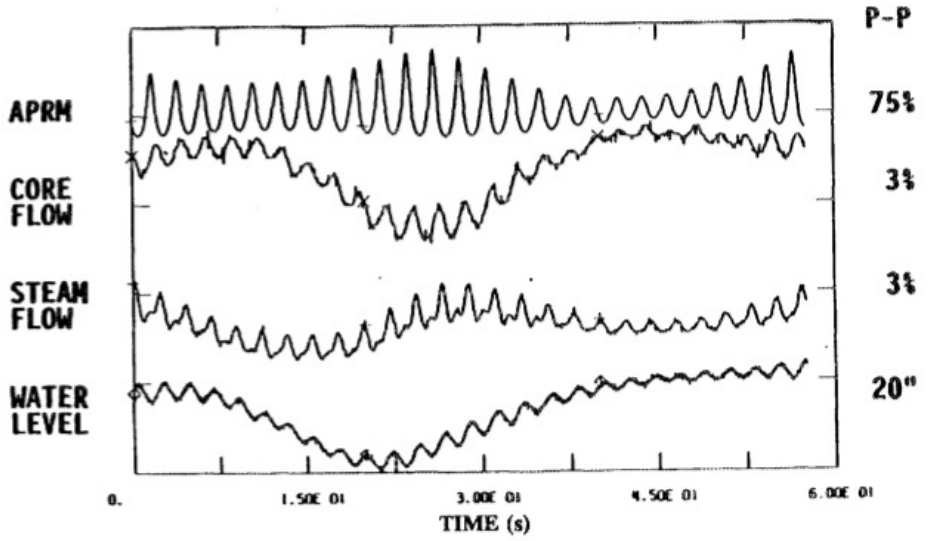

Figure 8: Example of an in-phase oscillation event: LaSalle reactor [March-Leuba, 1992].

Average void fraction Comparing two cores with different average void fraction, we would favor the lower void fraction core with respect to stability. Higher void fraction increases the neutronic feedback and have a larger two-phase pressure drop, where the latter yields stronger inlet flow feedback.

Inlet velocity A lower inlet velocity is followed by a longer time delay, which will emphasis the channel instability affecting the neutronic flux more. Note that the parametric effect of inlet velocity follows the reasoning presented earlier in section 3.2.4.

Axial power shape The axial power shape of the core tend to favor the case of bottom peaked power shapes with respect to instability. A bottom-peaked shape will create a higher average void fraction, leading to a more unstable system as reviewed above. As stated above, a higher average void fraction destabilizes the system.

Inlet subcooling In most cases, lowering the subcooling will lead to a destabilizing effect because it increases the operating power level.

3.4 DWO in an Electronics Cooling Loop

The following review is a summary of the research presented in Sun et al. [2009]. The tracker thermal control system (TTCS) is an active-pumped two-phase carbon dioxide cooling loop, designed to remove waste heat from front-end electronics of the so-called Alpha Magnetic Spectrometer (AMS). The AMS is a cosmic ray detector, planned to be operated on board the International Space Station. The TTCS will be the first active pump-driven two-phase thermal control system for space application. The two parallel evaporators, which consumes excessive heat from the AMS, must provide a stable and uniform thermal boundary condition to the electronics, and any irregularities in the evaporators are unacceptable. Two-phase flow behavior resembling DWO has been observed in the cooling loop.

At certain inlet subcooling and flow rate, experimental data showed oscillations in the outlet temperature of both evaporators. In figure 9, 10 and 11 various self-sustained oscillations are shown for constant subcooling and various pump rotation speeds controlling the system flow rate. The red and black lines indicate the outlet temperature of the top and bottom evaporators, respectively. The blue and green line represents the pressure drop in the top evaporator and the centrifugal pump, respectively.

By comparing the results shown in figure 11 with that of figure 9, the researchers observed that temperature oscillations were amplified with reduced flow rate. At an even lower flow rate (figure 10) dry-out was observed. As we review in section 3.2.4, the stability of a system experiencing DWO is reported to decrease as we reduce the flow rate. Sun et al. [2009] also found that by increasing the working pressure, the temperature oscillations became weaker, which again is supported by literature reviewed earlier. It was further shown that the self-sustained oscillation had a period approximately equal to the evaporator transit time, which is an indication of, at least according to that stated by Ambrosini et al. [2000], that what Sun et al. [2009] observed was in fact DWO at low subcooling operating conditions.

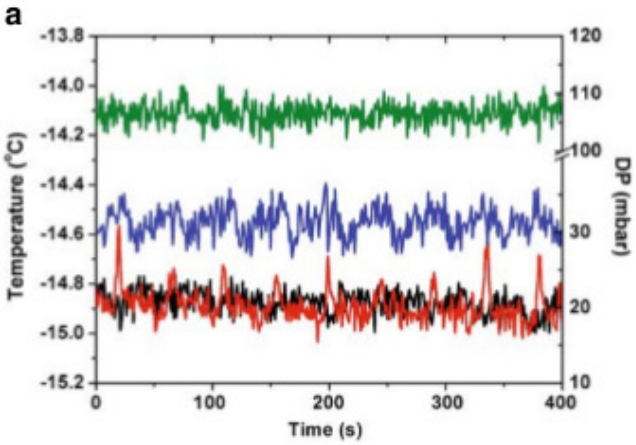

Figure 9: Observed sustained oscillations with pump speed equal 3300 RPM [Sun et al., 2009]. Red line: outlet temperature of the top evaporator, black line: outlet temperature of the bottom evaporator, blue line: pressure drop in the top evaporator, green line: pressure drop in centrifugal pump.

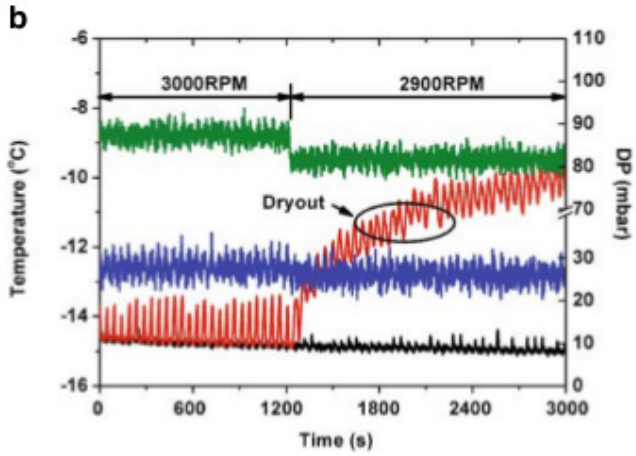

Figure 10: Dry-out occurs at the top evaporator for pump speed equal 2900 RPM [Sun et al., 2009]. Red line: outlet temperature of the top evaporator, black line: outlet temperature of the bottom evaporator, blue line: pressure drop in the top evaporator, green line: pressure drop in centrifugal pump.

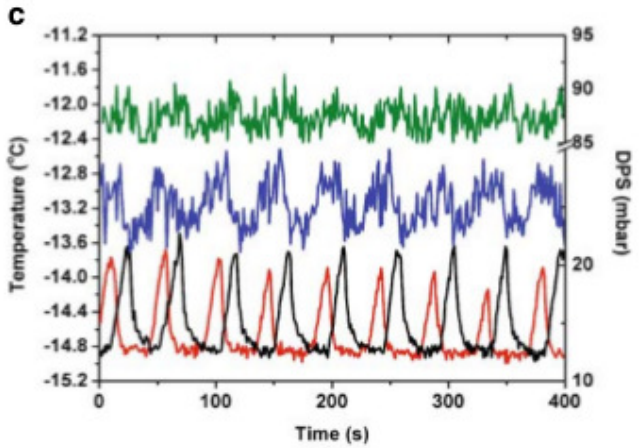

Figure 11: Observed sustained oscillations with pump speed equal 3000 RPM [Sun et al., 2009]. Red line: outlet temperature of the top evaporator, black line: outlet temperature of the bottom evaporator, blue line: pressure drop in the top evaporator, green line: pressure drop in centrifugal pump.

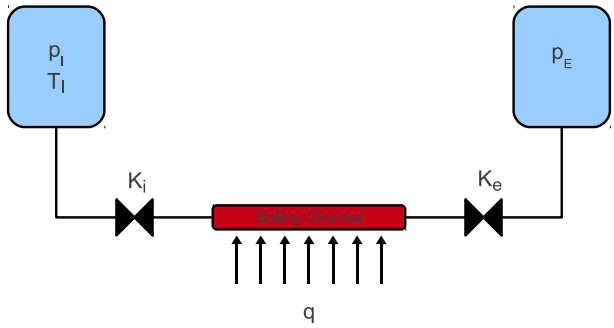

Figure 12: Schematic of the modeled system.

4 Modeled Density Wave Oscillations

4.1 Modeled System

The modeled system is shown in figure 12. The boiling channel is a circular horizontal pipe, heated with a constant uniform power q. The system is exposed to a constant externally imposed pressure drop Δp_{ext} given by the inlet- and exit pressure reservoirs, denoted by p_I and p_E, respectively. T_I represents the fluid inlet temperature. Two flow restrictions are placed at the channel inlet and exit with respective restriction coefficients K_i and K_e.

4.2 Model

4.2.1 Mathematical Model

The objective of the current model is to investigate the fundamental mechanisms of density wave oscillations at various levels of subcooling. The following assumptions are made concerning the mathematical description of the system flow:

1. One dimensional
2. Horizontal
3. Homogenous flow
4. Thermodynamic equilibrium
5. Constant externally imposed pressure drop
6. Constant inlet temperature

7. Constant uniform heating

The model solves the conservation equation for mass, momentum and energy as given in equation 36, 37 and 38, respectively:

$$\textit{Mass:} \qquad \frac{\partial \rho_m}{\partial t} + \frac{\partial G}{\partial z} = 0 \tag{36}$$

$$\textit{Momentum:} \qquad \frac{\partial G}{\partial t} + \frac{\partial}{\partial z}\left(\frac{G^2}{\rho_m}\right) = -\frac{\partial p}{\partial z} - \frac{f}{2D}\frac{G^2}{\rho_m} \tag{37}$$

$$\textit{Energy:} \qquad \frac{\partial h_m}{\partial t} + \frac{G}{\rho_m}\frac{\partial h_m}{\partial z} = \frac{1}{A\rho_m}\frac{q}{L} \tag{38}$$

which is similar to the system of equations given in section 2.2.1. However, the current system is regarded as horizontal and therefore, compared to equation 20, we have removed the term concerning gravitation in equation 37. In the above energy equation we neglect friction dissipation and flow work, and equation 38 becomes as found in Delmastro et al. [1991].

4.2.2 Numerical Scheme

The flow model utilizes the so-called *Space-Time Least-Square Spectral Element Method* (ST-LQSEM) in order to solve the governing equations (see equation 36, 37 and 38). To present the nature of the numerical scheme is outside the scope of work, and the reader is referred to de Maerschalck [2003] for more information.

4.2.3 Fluid Properties

Fluid properties are found using REFPROP8 (REference Fluid PROPerties v. 8.0) developed by the National Institute of Standards and Technology (NIST). The density is throughout the boiling channel regarded as a function of enthalpy only, assuming a constant channel pressure equal to that of the inlet pressure p_i found at steady state. Thus, $\rho_m = \rho_m(h_m, p_i)$. Other average fluid properties are found from the common mixture pressure and enthalpy obtained by solving the governing equations.

4.2.4 Restriction Pressure Drop

The inlet and exit flow restrictions are modeled using restriction coefficients K_i and K_e, respectively. Here, the pressure drop across each restriction is modeled as given in equation 39 and 40:

$$\Delta p_i = \frac{1}{2}K_i\frac{G_i^2}{\rho_{m,i}} = \frac{1}{2}K_i\rho_{m,i}u_{m,i}^2 \tag{39}$$

$$\Delta p_e = \frac{1}{2}K_e\frac{G_e^2}{\rho_{m,e}} = \frac{1}{2}K_e\rho_{m,e}u_{m,e}^2 \tag{40}$$

where $u_{m,i}$ [m/s] and $u_{m,e}$ [m/s] are the boiling channel inlet and exit mixture velocities, respectively. The inlet and exit mixture densities are denoted as $\rho_{m,i}$ [kg/m^3] and $\rho_{m,e}$ [kg/m^3], respectively. G_i [kg/m^{2}s] and G_e [kg/m^{2}s] are the inlet and exit mass fluxes, respectively.

4.2.5 Pressure Boundary Condition

The flow evolves from static state in the inlet reservoir, and the boiling channel inlet pressure p_i, is found as given in equation 41. The channel exit pressure p_e is determined in a similar manner by equation 42. We account for the change in dynamic pressure as the fluid mixture flows from and to the inlet and exit reservoirs, respectively. Equation 39 and 40 ensure that the inlet and exit pressure of the boiling channel evolve in accordance to the constant externally imposed pressure.

$$p_i = p_I - (\Delta p_i + \frac{1}{2}\frac{G_i^2}{\rho_{m,i}}) \tag{41}$$

$$p_e = p_E + (\Delta p_e - \frac{1}{2}\frac{G_e^2}{\rho_{m,e}}) \tag{42}$$

4.2.6 Modeling Procedure

In order to study density wave oscillations we are interested in the system's transient response from a steady state condition. Thus, we must ensure that our initial system conditions are in fact a steady state solution. The model script allows for the governing equation to be solved both as time-dependent (transient) and time-independent (steady-state). The latter is therefore simulated first, assuming a mass flux G and an exit pressure p_E as the system boundary conditions. The obtained steady state solution yields the necessary inlet reservoir pressure p_I. With the obtained steady state solution, we initiate the transient modeling, using the newly calculated inlet reservoir pressure p_I together with the previously assigned exit reservoir pressure p_E as boundary conditions. The boiling channel system is now exposed to an externally constant pressure drop $\Delta p_{ext} = p_I - p_E$, and the transient response of the system can be investigated. All results presented here are found for the same steady state mass flux and exit reservoir pressure p_E. According to the above described modeling procedure, we obtain, by varying the heated channel power q and/or the inlet temperature T_I, different inlet reservoir pressures p_I resulting from the steady state simulation. Hence, the various simulations will experience different Δp_{ext}.

The effect of subcooling on DWO is investigated by comparing self-sustained periodic oscillations, also referred to as marginally stable oscillations, obtained for different values of the subcooling number N_{sub}. As we reviewed in section 3.2, such oscillatory flow is found on the marginal stability threshold for the boiling system considered, separating the regions yielding converging and diverging flow behavior, respectively. Hence, the phase-change number N_{pch} will also differ for

each operating conditions. The marginally stable operating conditions compared in this work are found by changing the system's operating conditions as described above until a self-sustained periodic oscillation is found.

4.2.7 The Boiling Boundary

The boiling boundary location λ_b is defined as the boiling channel axial location where the bulk fluid temperature reaches the saturation temperature [Achard et al., 1985]. With the model presented in this thesis it was not possible to investigate the oscillations in the boiling boundary location in detail due to the lack of an explicit expression. In the literature (e.g. Rizwan-Uddin and Dorning [1986] and Rizwan-Uddin [1994]), two-phase flow models are presented which give such an explicit expression for the change in λ_b as a function of time. However, in the following section the author will explain how an assumed valid expression for the transient behavior of the boiling boundary location $\lambda_b(t)$ was obtained here. The final expression is only applied to self-sustained periodic oscillations (marginally stable oscillations).

In section 3.2 theory regarding stability maps of boiling two-phase flow systems was reviewed. In the stability map given in figure 3, the solid blue line separates the *Single-phase liquid* operating region from the *Stable* two-phase flow region, and consequently represents steady state operating conditions that yield a boiling boundary located at the channel exit ($\lambda_b = L$ where L is the channel length). On this line $N_{sub}/N_{pch} = 1$. Similar lines representing any constant arbitrary boiling boundary can be expressed as given in equation 43:

$$N_{sub} = \frac{\lambda_b}{L} N_{pch} \tag{43}$$

Figure 28 shows such lines of constant boiling boundary location as a part of the investigation of the modeled results. By rearranging equation 43 we can obtain an expression for λ_b as shown in equation 44:

$$\lambda_b = \frac{N_{sub}}{N_{pch}} L \tag{44}$$

which is valid for steady state operating conditions.

When a boiling channel system experiences oscillations, the phase-change number N_{pch} will vary because $N_{pch} \propto 1/G_i$, where G_i is the boiling channel inlet mass flux. The equation for N_{pch} is given in equation 31. It is now assumed that equation 44 yields also when N_{pch} varies in time (N_{sub} is constant during transients). The boiling boundary equation given in equation 44 consequently becomes a function of time. However, oscillations in λ_b are time delayed with respect to the variations in G_i. Equation 44 will only provide us with the possible values of λ_b independent of when they occur. Equation 45 shows how the location of the boiling boundary can be expressed when taking into account a time delay δ:

$$\lambda_b(t) = \frac{N_{sub}}{N_{pch}(t-\delta)} L \tag{45}$$

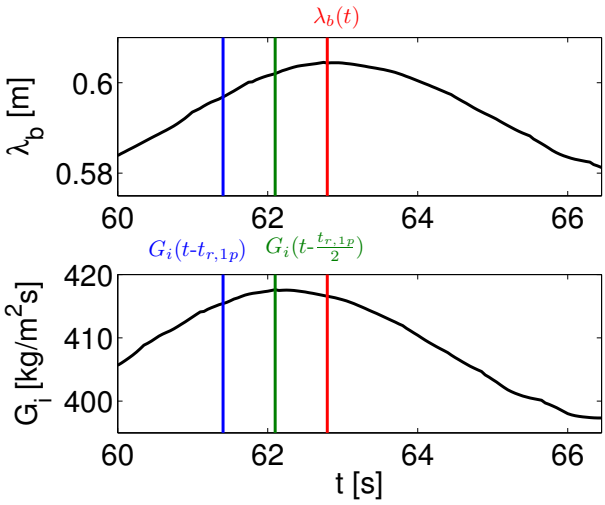

Figure 13: The developed expression for oscillations in the boiling boundary versus oscillations in inlet mass flux. Blue line: fluid enters channel, Green line: G_i reach maximum value, Red line: fluid leaves the single-phase region.

The next step is to determine a valid time delay δ in the boiling boundary oscillations with respect to the oscillations in N_{pch} which the modeled results will provide. In a boiling channel system, where the fluid is heated with constant uniform heat, the single-phase residence time $t_{r,1p}$ is constant even during transients [Rizwan-Uddin, 1994, Rizwan-Uddin and Dorning, 1986]. This is the case for our modeled system. Details regarding residence time can be found in section 4.2.8. The mass flux in the entire single-phase region is always equal to the value of G_i because the density is assumed to be constant throughout the region. Since a fluid particle always spends a constant time $t_{r,1p}$ in the single-phase region, the maximum value in λ_b, denoted here as λ_b^{max}, must be due to fluid that experience the maximum possible average mass flux as it progresses through the single-phase region. In other words, the fluid that is moving faster needs more space to reach the saturation point. The fluid that leaves the single-phase region when $\lambda_b = \lambda_b^{max}$ must therefore be the fluid that enters the channel at a time $\frac{t_{r,1p}}{2}$ before the time of the maximum value in G_i. Figure 13 is added to clarify the above. Hence, the proper time delay is $\delta = \frac{t_{r,1p}}{2}$, and the final expression for the time delayed boiling boundary location as a function of N_{pch} is given in equation 46:

$$\lambda_b\left(t\right) = \frac{N_{sub}}{N_{pch}\left(t - \frac{t_{r,1p}}{2}\right)} L \tag{46}$$

In figure 14, we compare the explicit expression for $\lambda_b(t)$ given in equation 46 with one of our modeled results. The modeled boiling boundary location is represented by the rapid change seen in the mixture density at the intersection

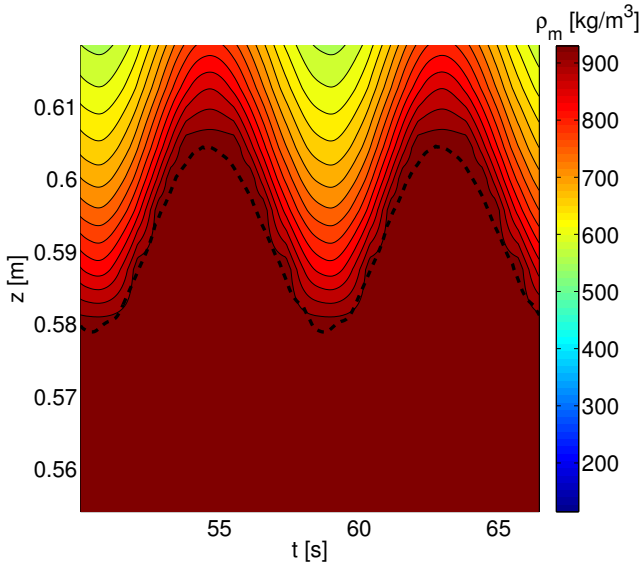

Figure 14: Comparison of the explicit expression for λ_b (dashed line) and the modeled intersection between the single-phase region and the two-phase region.

between the single-phase region and the two-phase region. The derived explicit expression for λ_b fits reasonably well with how the flow model determines the boiling boundary location.

4.2.8 Boiling Channel Residence Time

This section presents how the boiling channel residence time is defined. The equations that follow are solved numerically using the modeled results. The boiling channel residence time t_r [s] is defined as the time the mixture spends in the boiling channel when traveling from the inlet to the exit. The boiling channel residence time of a mixture entering the channel at a time t [s] can be expressed mathematically as:

$$t_r(t) = \int_{z=0}^{z=L} \frac{dz}{u_m(z, t+\delta(z))} \tag{47}$$

where z [m] is the axial location of the mixture with respect to the channel inlet, and L [m] is the boiling channel length. $u_m(z, t+\delta(z))$ [m/s] is the mixture velocity at a distance z from the inlet at a time $t+\delta(z)$, where $\delta(z)$ is the time the mixture has spent in the channel when reaching z. Hence, $t_r = \delta(L)$. The mean boiling channel residence time $\bar{t}_r$ [s] is given as:

$$\bar{t}_r = \frac{1}{t_p} \int_{\beta=t}^{\beta=t+t_p} t_r(\beta) d\beta \tag{48}$$

where t_p [s] is the oscillation period.

The single-phase residence time $t_{r,1p}$ [s] is the time the subcooled liquid spends in the single-phase region. In a boiling channel system where the fluid is heated with constant uniform heat, the single-phase residence time is constant even during transients [Rizwan-Uddin, 1994, Rizwan-Uddin and Dorning, 1986]. In order to calculate the single-phase residence time we apply the explicit expression for the location of the boiling boundary $\lambda_b(t)$ given in equation 46. Using equation 46, we express the mean boiling boundary location $\bar{\lambda}_b$ [m] as:

$$\bar{\lambda}_b = \frac{1}{t_p} \int_{\beta=t}^{\beta=t+t_p} \lambda_b(\beta) d\beta \tag{49}$$

From the above equation, the always constant single-phase residence time $t_{r,1p}$ is found as:

$$t_{r,1p} = \frac{\bar{\lambda}_b}{\bar{u}_{m,i}} \tag{50}$$

where $\bar{u}_{m,i}$ [m/s] is the mean mixture inlet velocity, and is defined as in equation 51:

$$\bar{u}_{m,i} = \frac{1}{t_p} \int_{\beta=t}^{\beta=t+t_p} u_{m,i}(\beta) d\beta \tag{51}$$

The mean two-phase residence time $\bar{t}_{r,2p}$ [s] is the time the mixture spends in the two-phase region, and is found by the relation given in equation 52:

$$\bar{t}_{r,2p} = \bar{t}_r - t_{r,1p} \tag{52}$$

4.3 Validating the Model

The two-phase flow model presented in this thesis has been validated by comparing the modeled results to relevant findings presented in the literature. The comparing literature will be specified as the validation is made.

4.3.1 Modeled Stability Map

Operating conditions showing close to marginally stable oscillations has been found in different regions of parameter space. Such oscillations are neither converging (stable) or diverging (unstable), but oscillate with a finite period and amplitude. The reader is referred to section 4.2.6 for information regarding how the modeled stability map was obtained. The stability map found for the system considered here is shown in figure 15, together with the theoretical stability threshold of Guido et al. [1991] and the simplified stability criteria of Ishii [1971] (see section 3.2). Our modeled stability threshold, and its relation to the these theoretical thresholds is the first sign of result validity. If we compare figure 15 to that of figure 5, it is obvious that our equilibrium flow model provides a stability threshold which shows a similar relationship to the Guido et al. [1991] threshold and the simplified

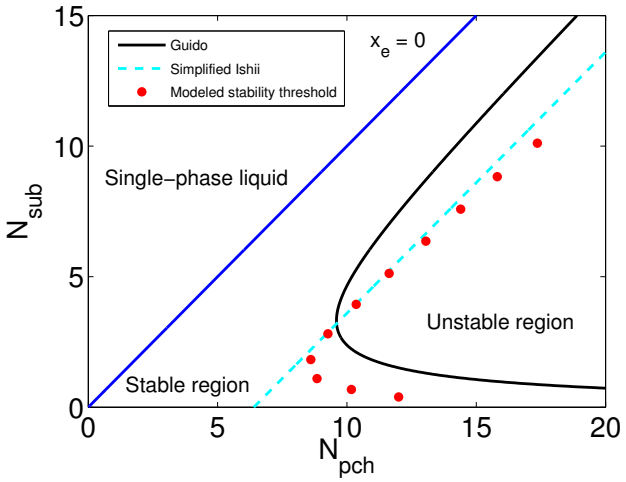

Figure 15: Modeled stability map versus the stability threshold of Guido et al. [1991] and the simplified stability criteria of Ishii [1971].

Label	T_I[K]	q[W]	N_{sub}	N_{pch}
Low Subcooling	380	166.5	0.4	12
Intermediate Subcooling	378	124.5	2.8	9.3
High Subcooling	375	233	10.1	17.4

Table 1: System inlet temperature and applied heat for the operating points given in figure 16.

stability threshold of Ishii [1971] as that of the equilibrium theory threshold (red line) shown in figure 5.

4.3.2 Oscillation Period versus Channel Residence Time

To further ensure the validity of our two-phase flow model, we compared some of our results with the findings of Rizwan-Uddin [1994] and Ambrosini et al. [2000]. As reported by Rizwan-Uddin [1994], and later confirmed by Ambrosini et al. [2000], DWO shows a significant difference in the observed oscillation period versus boiling channel residence time. In Ambrosini et al. [2000] it was concluded that this ratio was depending on the level of system subcooling. Consequently, it was in this section found convenient to label three of our marginally stable operating conditions according to their respective level of subcooling, and hence the scaling parameter N_{sub}. The selected operating points and their respective labels are shown in figure 16. In table 1, the applied inlet temperatures and heat loads are listed.

The modeled oscillations in inlet velocity for the three selected operating points are given in figure 17, 18 and 19, respectively. The vertical dotted lines indicate the *start* and *end* of a periodic oscillation, and these timespans will in future be

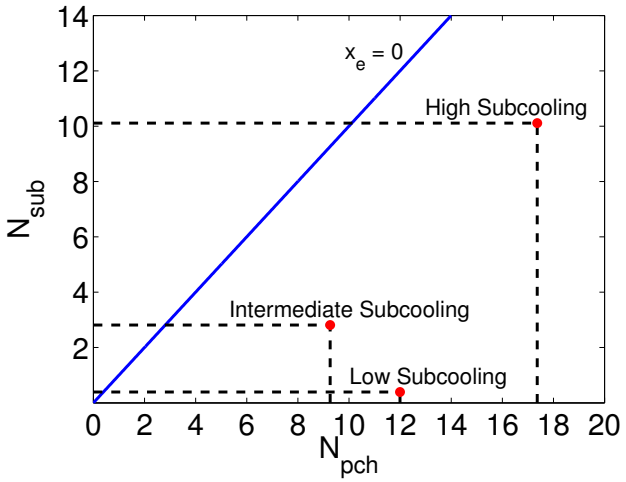

Figure 16: Selected marginally stable operating conditions.

Label	t_p[s]	$\bar{t}_r$[s]	$t_p/\bar{t}_r$
Low Subcooling	0.81	0.59	1.4
Intermediate Subcooling	2.5	1.25	2.0
High Subcooling	8.15	1.68	5.0

Table 2: Oscillation period t_p and mean boiling channel residence time $\bar{t}_r$ for operating points given in figure 16.

used to investigate the respective system behavior. The oscillation period t_p and the mean boiling channel residence time $\bar{t}_r$ are for the selected operating points as listed in table 2 together with the ratio $t_p/\bar{t}_r$. The reader is referred to section 4.2.8 for information regarding how the channel residence time is obtained. The ratio $t_p/\bar{t}_r$ is for the case of *Low Subcooling* and *Intermediate Subcooling* in accordance to the classical description of DWO where the oscillation period is believed to be approximately one to two times the boiling channel residence time [Boure et al., 1973]. For the case of *High Subcooling* this ratio is 5. The latter confirms what was addressed in Rizwan-Uddin [1994] regarding the increased ratio found at higher subcooling. The observed change in the ratio $t_p/\bar{t}_r$ is, as also stated by Ambrosini et al. [2000], clearly an effect of the level of applied system subcooling. The two-phase flow model applied here is from the above comparison able to show the change in oscillation period versus boiling channel residence time as found in the literature.

4.3.3 Strength of Density Waves

Rizwan-Uddin [1994] raised criticism towards the classical description of density wave oscillations partly because he observed DWO even when there was only a

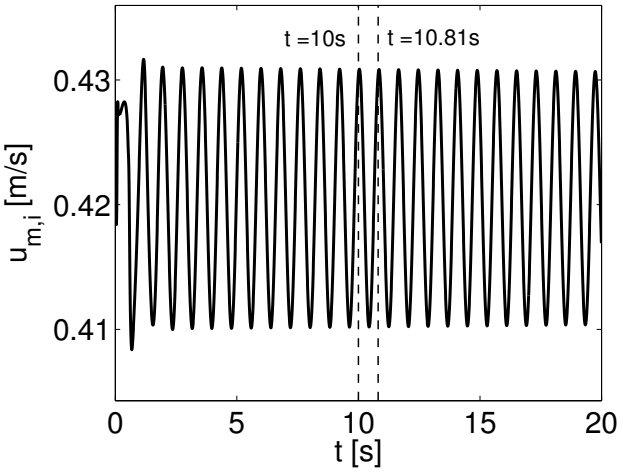

Figure 17: Oscillations in inlet velocity for the case of *Low Subcooling*.

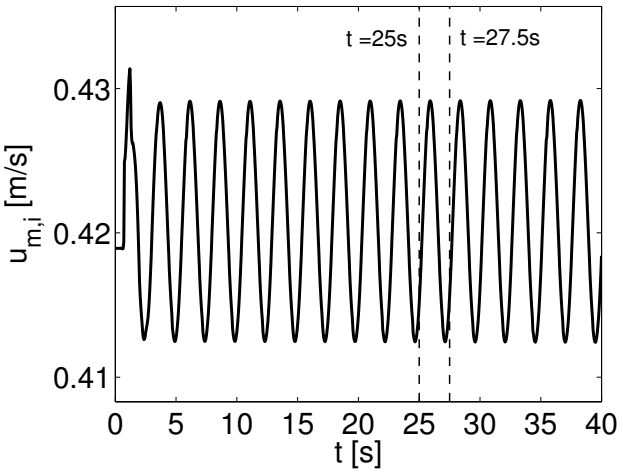

Figure 18: Oscillations in inlet velocity for the case of *Intermediate Subcooling*.

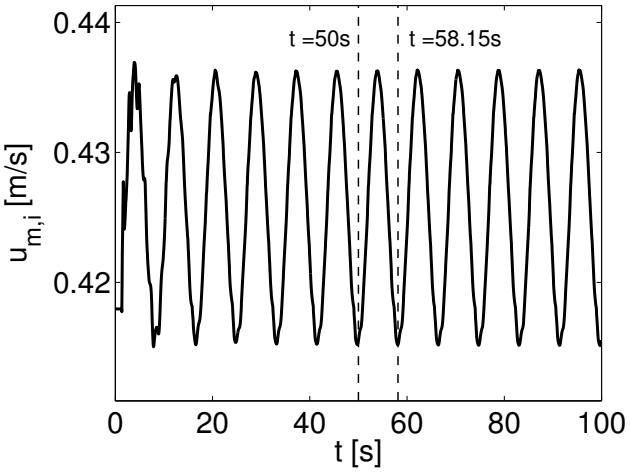

Figure 19: Oscillations in inlet velocity for the case of *High Subcooling*.

"weak" density wave present in the boiling channel. This finding, in addition to other, led Rizwan-Uddin [1994] to doubt the importance of density waves with respect to the occurrence of DWO. In figure 20, 21 and 22, the oscillations in mixture density are shown for selected locations in the two-phase region of the boiling channel. Each of the above given figures represents one of the three earlier labeled operating points. As indicated by the marked maximum values (blue dots), there is clearly a density wave present for all three levels of subcooling. The phenomenon of a density wave can easily be explained from the fact that the exit ($z = 1.0$m), always feels the effect of an inlet perturbation at a later time than for instance $z = 0.7$m. The "strength" of a density wave is according to Ambrosini et al. [2000] due to the relationship between the time needed to propagate density waves and the oscillation period. Hence, for low subcooling we should see a stronger density wave than in the case of higher subcooling because of the lower ratio $t_p/\bar{t}_r$. This can be confirmed by comparing figure 20 (*Low Subcooling*) with figure 22 (*High Subcooling*). The time delay between the maximum value of $z = 0.7$ m and $z = 1.0$ m make up a much larger portion of the oscillation period in the former than in the latter. The same is true for *Intermediate Subcooling* with respect to *High Subcooling*. The flow model's ability to qualitatively describe the variation in density wave strength is taken as a sign of validity of the present model.

4.3.4 Density versus Velocity

Rizwan-Uddin [1994] discovered that in the case of higher system subcooling, the oscillations found in the exit restriction pressure drop were governed more by the variation in exit mixture velocity than by density. Ambrosini et al. [2000] confirmed this, but added that for low system subcooling we would see the opposite. Both

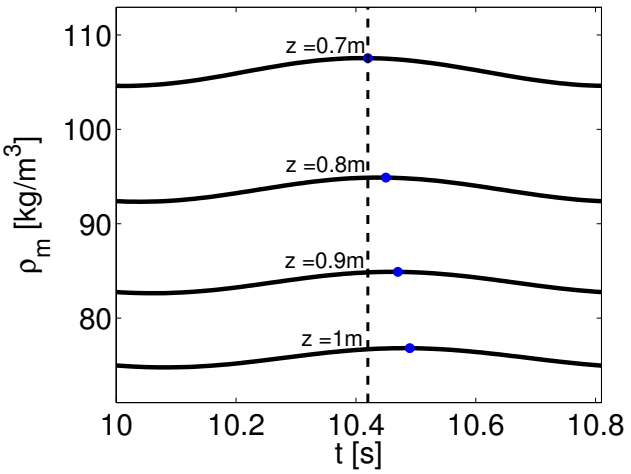

Figure 20: Oscillations in mixture density for *Low Subcooling*.

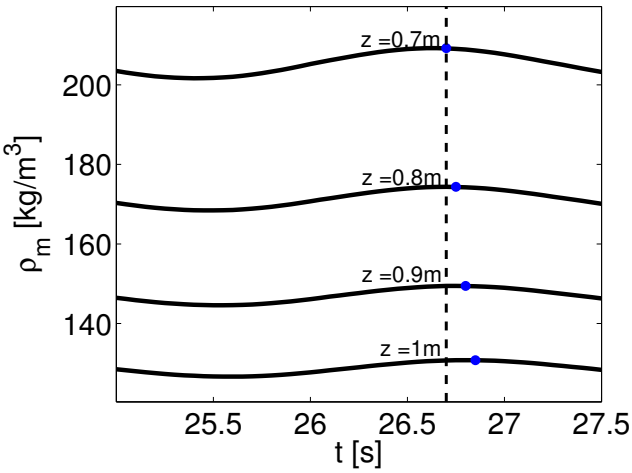

Figure 21: Oscillations in mixture density for *Intermediate Subcooling*.

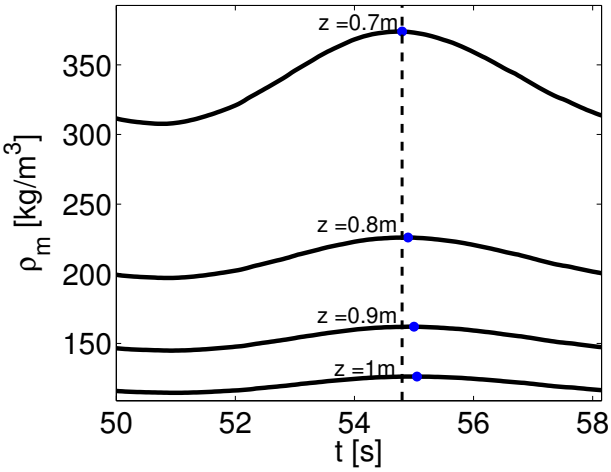

Figure 22: Oscillations in mixture density for *High Subcooling*.

of these findings have been replicated here. The behavior of an exit restriction is important in boiling channel systems because it in most cases is the largest system source of pressure drop, and is the most time delayed system pressure drop component, which consequently gives it the strongest effect on the boiling channel inlet. Figure 23, 24 and 25 show how the exit restriction pressure drop (Δp_e) vary with respect to the exit mixture velocity ($u_{m,e}$) and density ($\rho_{m,e}$). In figure 23, which represents *Low Subcooling*, the variation in exit restriction pressure drop is highly governed by the variation in exit density, with Δp_e moving almost in-phase with $\rho_{m,e}$. $u_{m,e}$ is almost 180°out-of-phase with respect to Δp_e. At *Intermediate Subcooling*, shown in figure 24, Δp_e is still more in-phase with $\rho_{m,e}$ compared to $u_{m,e}$. Turning to figure 25, we see that for *High Subcooling* the exit restriction pressure drop is governed mostly by the variation in exit mixture velocity. The above confirms that the pressure drop in the exit restriction is governed by variations in mixture density at lower subcooling, and that it is shifted towards variations in mixture velocity as the level of subcooling is increased. As also Ambrosini et al. [2000] discovered, the relative weight of either mechanism is different depending on the parameter space considered.

4.4 Modeled Result

Now that we have validated the two-phase flow model presented in section 4.2 with the results of Rizwan-Uddin [1994] and Ambrosini et al. [2000], we will move on to investigate the modeled results further. The results presented in the following section are all for marginally stable operating conditions obtained by applying the constant system conditions given in table 3. The modeling procedure is reviewed in section 4.2.6. The modeled stability map presented earlier is revisited in figure

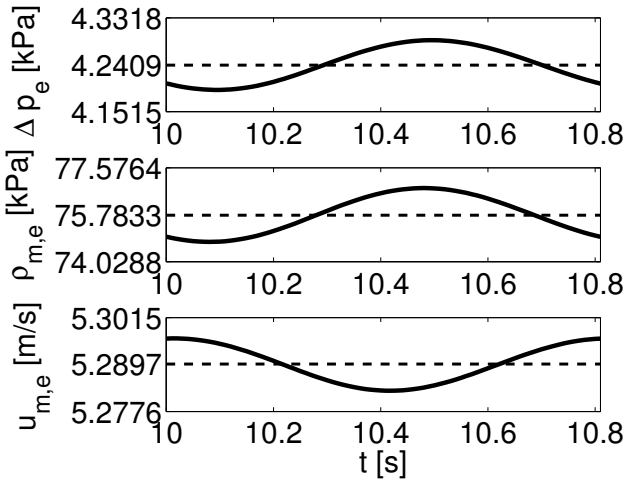

Figure 23: Oscillations in exit restriction pressure drop (Δp_e) versus exit mixture density ($\rho_{m,e}$) and exit mixture velocity ($u_{m,e}$) at *Low Subcooling*.

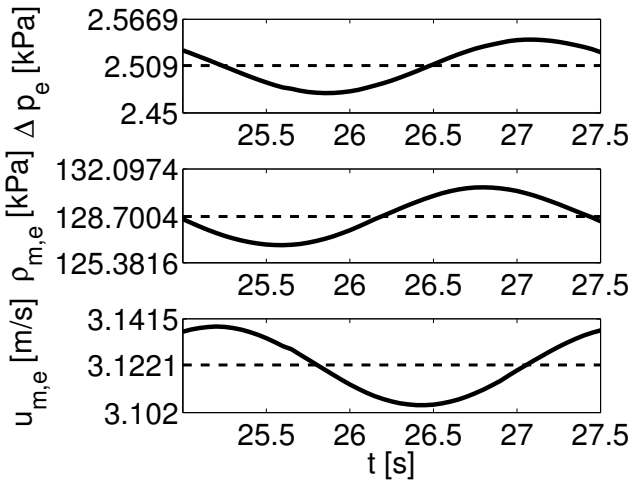

Figure 24: Oscillations in exit restriction pressure drop (Δp_e) versus exit mixture density ($\rho_{m,e}$) and exit mixture velocity ($u_{m,e}$) at *Intermediate Subcooling*.

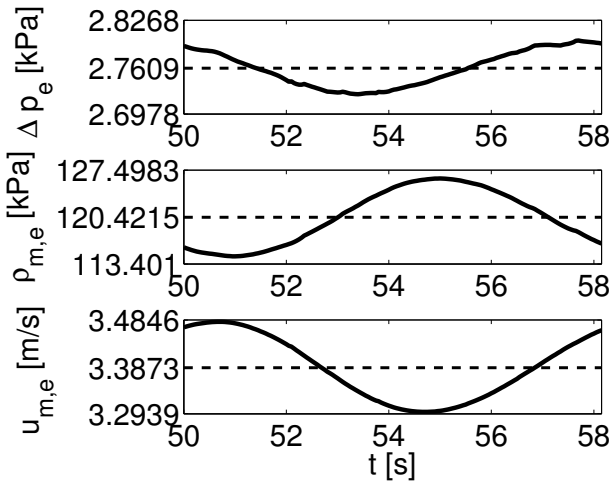

Figure 25: Oscillations in exit restriction pressure drop (Δp_e) versus exit mixture density ($\rho_{m,e}$) and exit mixture velocity ($u_{m,e}$) at *High Subcooling*.

Fluid:	Water
Channel length:	$L = 1$ m
Channel diameter:	$D = 0.005$ m
Inlet restriction:	$K_i = 12$
Exit restriction:	$K_e = 4$
Exit reservoir pressure:	$p_E = 120$ kPa
Steady state mass flux:	$G = 400$ kg/m^{2}s

Table 3: Constant system conditions from which presented results are obtained.

26. As shown, the operating points yielding the stability threshold are labeled with numbers signifying a higher level of subcooling. These labels will be used in the following analysis of the modeled results. However, the previously defined labels *Low Subcooling*, *Intermediate Subcooling* and *High Subcooling* given in figure 16, now represented by operating condition 1,5, and 11 in figure 26, respectively, are still valid and will be referred to when convenient.

4.4.1 The Boiling Boundary

The boiling boundary location λ_b is defined as the channel axial location where the bulk fluid temperature reaches the saturation temperature [Achard et al., 1985]. The reader is referred to section 4.2.7 for information regarding how the transient behavior of λ_b is determined. Figure 27 shows the evolution of the mean boiling boundary location $\bar{\lambda}_b$ as we move along the stability threshold towards higher subcooling. The mean boiling boundary is continuously moved downstream towards what seems to be a maximum limit $\bar{\lambda}_b^{max}$. With the use of a slope curve fit, this

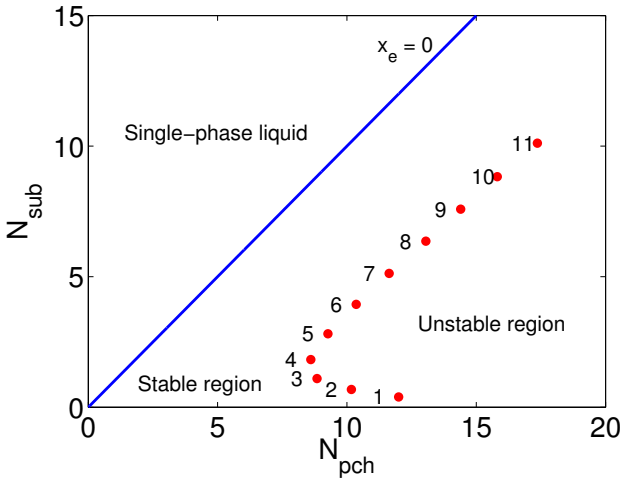

Figure 26: Modeled stability map with new labels.

maximum value is assumed to be $\bar{\lambda}_b^{max} = 0.6$m. The postulate of an upper limit in $\bar{\lambda}_b$ can be illustrated by plotting lines in a stability map that represent operating conditions yielding a constant $\bar{\lambda}_b$. For our modeled system, such operating lines are found using equation 43 with $L = 1.0$m. Figure 28 shows a selection of lines with constant $\bar{\lambda}_b$ plotted in the modeled stability map. The modeled stability threshold seems to approach the red dotted line yielding $\bar{\lambda}_b^{max} = 0.6$m, but this should be investigated in future work. The black dotted lines represent mean boiling boundary locations corresponding to that of their respectively intersected operating point. Again, the solid blue line indicates a boiling boundary located at channel exit. From figure 28, it is evident that the mean boiling boundary of any operating point moves downstream towards the exit as the system operating condition moves closer the *Single-phase liquid* region. By discovering that the stability threshold seems to approach a maximum mean boiling boundary limit we realize that if we can ensure that our modeled system will operate with $\bar{\lambda}_b > \bar{\lambda}_b^{max}$, we can be sure that the system will never enter the unstable region independent of the applied level of system subcooling. However, the practical application of such a discovery is not investigated further.

In boiling channel systems where the fluid is heated with constant uniform heat flux, the residence time in the single-phase region is constant even during transients [Rizwan-Uddin, 1994]. Since the subcooled liquid always spends an equal amount of time in the single-phase region for any given operating condition, the maximum axial location of the λ_b is due to a fluid particle that experiences the highest possible average velocity as it progresses through the single-phase region. This maximum value is represented by λ_b^{max}. In figure 29 we see how the amplitude in λ_b changes as we move along the stability threshold towards higher subcooling. At lower subcooling, the slope of the outlined path, given by the operating conditions

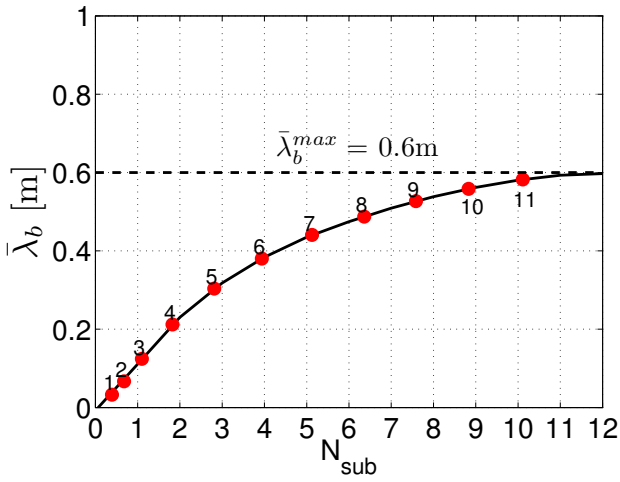

Figure 27: Mean boiling boundary location $\bar{\lambda}_b$ for marginally stable oscillations at different levels of subcooling.

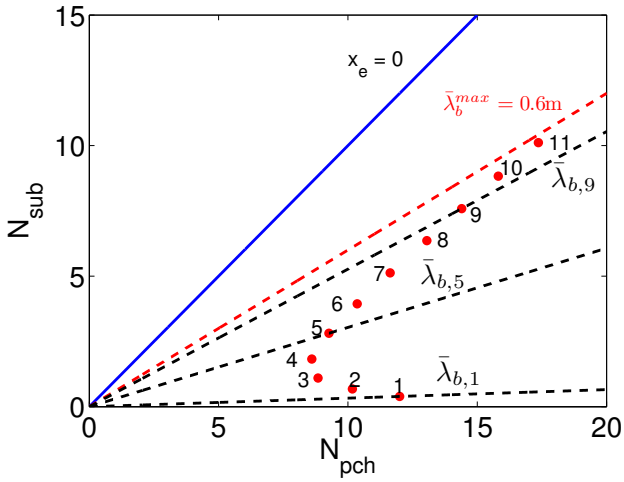

Figure 28: Modeled stability map with lines indicating constant mean boiling boundary $\bar{\lambda}_b$.

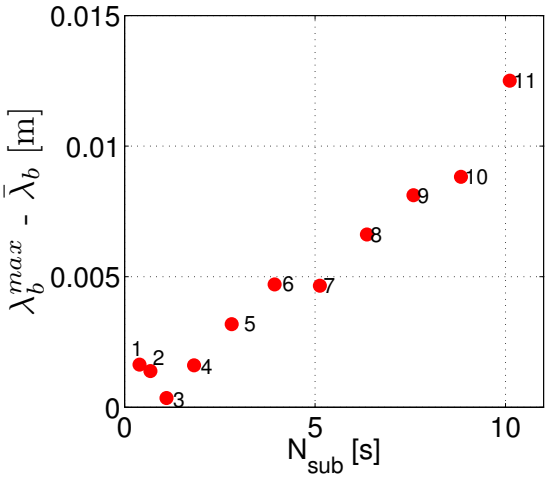

Figure 29: Amplitude of the oscillation in boiling boundary location λ_b for marginally stable oscillations at different levels of subcooling.

1, 2 and 3, is negative, implying that the amplitude of the oscillations in λ_b is reduced. However, the mean boiling boundary location for the respective operating conditions is moved downstream as shown earlier in figure 27. Going back to the modeled stability map given in figure 26, we can conclude that the observed decrease in the amplitude of λ_b in this low subcooled region, is due to a reduction in the system phase-change number N_{pch}. At higher levels of subcooling (operating point 4 to 11), the amplitude of λ_b increases and seems to increase exponentially as we move closer to operating conditions yielding a mean boiling boundary location equal to $\bar{\lambda}_b^{max} = 0.6$m.

4.4.2 Oscillations in Density and Velocity

As the level of system subcooling is increased, there is a shift from mixture density towards mixture velocity when it comes to controlling the exit restriction pressure drop (see section 4.3.4). Figure 30 and 31 shows the change in oscillation amplitude of the exit mixture density and exit mixture velocity, respectively, as we move along the stability threshold towards higher levels of subcooling. $\rho_{m,e}^{max}$ and $u_{m,e}^{max}$ denotes the maximum value in exit mixture density and exit mixture velocity, respectively. The amplitude in $\rho_{m,e}$ and $u_{m,e}$ increases continuously towards higher subcooling, with an almost exponential growth in both at a sufficiently high level of subcooling. Operating condition 7 appears to deviate from the outlined path, but the reason for this has not been discovered.

The growth in the amplitude of exit mixture density is here thought to be a combined effect of the boiling channel density profile and the amplitude of the boiling boundary location. The schematics shown in figure 32 will be used to try to

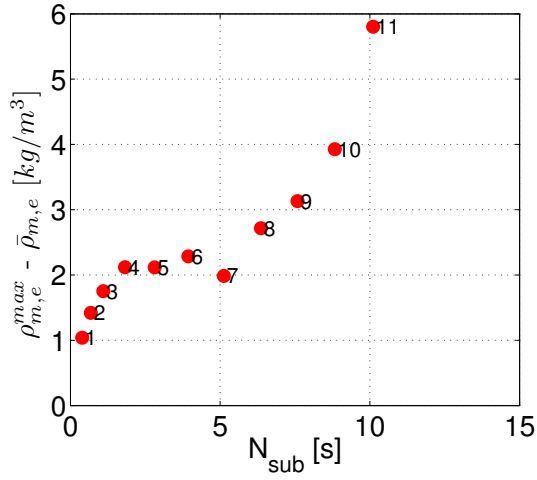

Figure 30: Amplitude of the oscillation in exit mixture density $\rho_{m,e}$ for marginally stable operating conditions at different levels of subcooling.

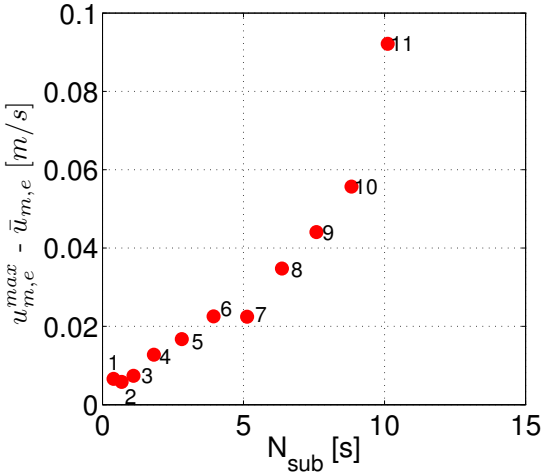

Figure 31: Amplitude of the oscillation in exit mixture velocity $u_{m,e}$ for marginally stable operating points at different levels of subcooling.

simplify the analysis that follows. Figure 32 shows the boiling channel density profile of two random imaginary operating conditions which for the sake of simplicity yield the same mean boiling boundary location $\bar{\lambda}_b$ and the same maximum boiling boundary location λ_b^{max}. Their difference lies in the slope of the boiling channel density profile. The bottom schematic represents an operating condition where the slop close to the exit is almost horizontal. The effect of a shift in the boiling boundary location from $\bar{\lambda}_b$ to λ_b^{max} will consequently produce only a small change in exit mixture density denoted by $\Delta\rho_{m,e}$. As explained in section 4.3, the effect of an oscillation in the boiling boundary location on exit mixture density will not happen instantaneously. Changes in downstream mixture density are propagated with the mixture velocity, and is seen as the so-called density wave. However, the effect of a change in λ_b will eventually present itself at the exit, but with a time delay equal to the two-phase region residence time. For the case of a steeper exit density profile as shown in the top schematic of figure 32, the change in mixture density will be larger due to the steeper exit slope. In figure 33 we show the steady state density profiles for the two operating conditions labeled earlier as *Low Subcooling* and *High Subcooling*. If we take into account the steeper slope and the larger amplitude in λ_b for the case of *High Subcooling* compared to *Low Subcooling*, we realize why the amplitude of $\rho_{m,e}$ must be higher in the former compared to the latter (see figure 30).

The observed oscillations in mixture velocity is a consequence of mass conservation which states that the amount of fluid entering and leaving the channel at any given time t must be the same. In the single-phase region, the velocity at a time t is constant due to the constant density. However, in the two-phase region the mixture density is reduced downstream of the boiling boundary location, and the mixture velocity must therefore increase towards the exit in order to uphold mass conservation. In figure 29 we showed that the amplitude of λ_b grew exponentially as the level of subcooling was increased. A consequence the latter is that a bigger channel region will be experiencing both single-phase and two-phase flow during one marginally stable oscillation. Hence, the two-phase mixture velocity must consequently oscillate more about its mean value. If we compare figure 31 and 29, we see that the above argument is valid for operating condition 4 to 11. For operating condition 1,2, and 3 there is a decrease in the amplitude of λ_b while the amplitude of $u_{m,e}$ remains almost constant. The latter is believed to be a result of the changes that occur in the channel density profile when the mean boiling boundary location is moved downstream (see figure 27). The density distribution in the two-phase region will have an effect on how mixture velocity evolves to uphold mass conservation. A further consequence of mass conservation is that u_m will vary in-phase throughout the two-phase region. This is illustrated in figure 34, where the oscillations in mixture velocity downstream of the boiling boundary location is plotted for a selection of axial channel locations. As shown, the mixture velocity varies in-phase, and implies that a change in λ_b will produce instantaneous changes in u_m towards the channel exit, and hence affect the exit restriction immediately. This is in contrast to what was shown in figure 22, where the effect of a change in λ_b with respect to mixture density was propagated downstream with a finite velocity

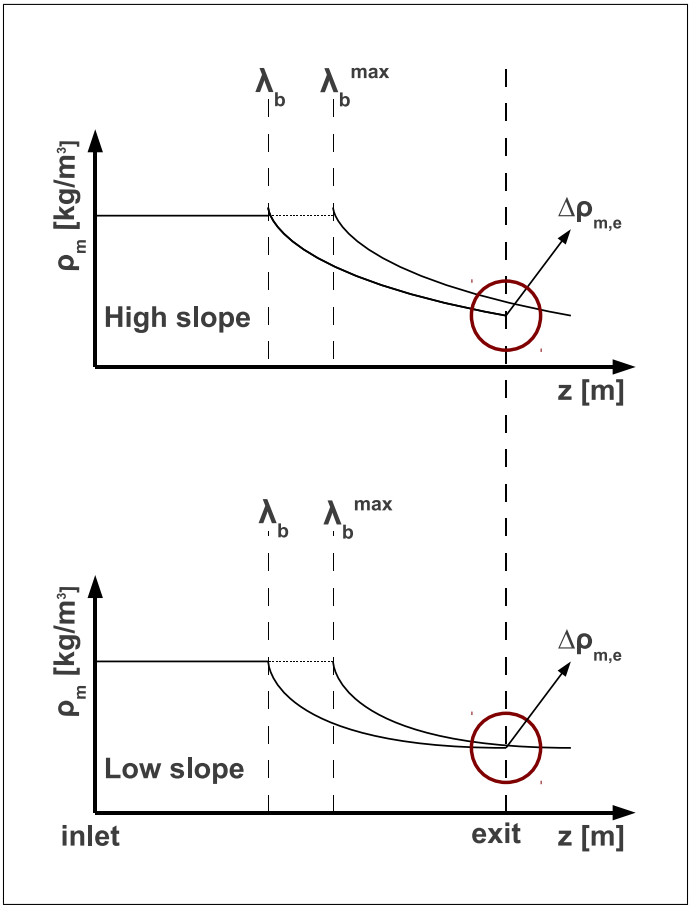

Figure 32: Schematic representation of the effect of density profile slope on the amplitude of exit mixture density oscillation.

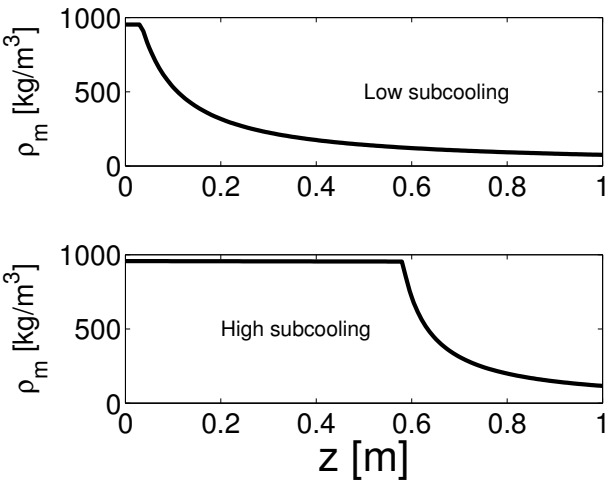

Figure 33: Steady state density profile for the *Low Subcooling* and *High Subcooling* operating conditions.

given by u_m. In section 4.3.4 we found that for higher levels of subcooling the exit restriction pressure drop was governed by oscillations in exit mixture velocity. Hence, for higher subcooling there is no time delay in the two-phase region with respect to changes in mixture velocity, and the time that it takes for an inlet perturbation to affect the exit is taken only as the single-phase residence time. How this will affect the dynamic response of the system is unclear, but it is nonetheless an interesting result.

In section 4.3.4 we found that for higher levels of subcooling the exit restriction pressure drop is governed more by the variations in exit mixture velocity than exit mixture density. The pressure drop across the exit restriction is governed by the relation given in equation 40. Hence, Δp_e is proportional to the exit mixture density as well as to the square of the exit mixture velocity. This relation states that the exit restriction pressure drop is more sensitive to a change in velocity than in density. As shown in figure 30 and 31, the amplitude in both $\rho_{m,e}$ and $u_{m,e}$, respectively, grows as the level of system subcooling is increased. However, because of the squared relationship between Δp_e and $u_{m,e}$, the mixture velocity becomes dominating at higher subcooling. At lower subcooling it is the variation in $\rho_{m,e}$ that causes the oscillation in Δp_e. This shift from a density dominated exit restriction towards a velocity dominated exit restriction is shown in figure 35, 36 and 37 for the earlier defined operating conditions *Low Subcooling*, *Intermediate Subcooling* and *High Subcooling*, respectively. The data presented in figure 35, 36 and 37 shows the oscillation Δp_e, $\rho_{m,e}$ and $u_{m,e}$ with respect to their mean value. In figure 35 we observe that $u_{m,e}$ barely changes, and it is consequently the variation in $\rho_{m,e}$ that causes the oscillation in Δp_e. For the case of *Intermediate Subcooling* the oscillation in $u_{m,e}$ grows noticeably stronger. However, the oscillation in $u_{m,e}$ is still

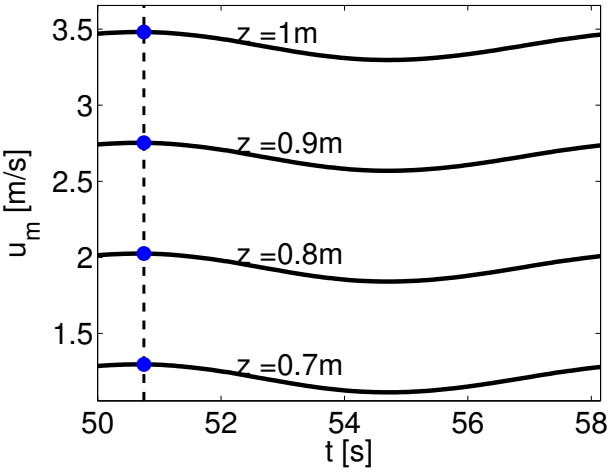

Figure 34: Oscillations in mixture velocity for the case of *High Subcooling*.

not strong enough to fully control the exit restriction pressure drop which is still more in-phase with $\rho_{m,e}$. In figure 37, which represents the *High Subcooling* case, the variation in $u_{m,e}$ is dominant with respect to Δp_e even though the oscillation in $\rho_{m,e}$ also grows stronger compared to the lower subcooling levels. This effect is due to the squared relationship between Δp_e and $u_{m,e}$, and it seems as though there is a smooth change towards a more velocity dominated exit restriction as the level of subcooling is increased.

4.4.3 Oscillation Period versus Boiling Channel Residence Time

The marginally stable operating conditions composing the modeled stability threshold showed a significant difference in the observed oscillation period. Figure 38 shows how the oscillation period t_p evolves as the subcooling is increased. The oscillation period increases almost linearly up to $N_{sub} \approx 5$. From this point on, t_p evolves in what seems to be an exponential manner. Hence, marginally stable operating conditions with N_{sub} sufficiently exceeding our maximum value will have an oscillation period that grows out of proportions.

In contrast to the exponential growth of t_p, the mean boiling channel residence time $\bar{t}_r$ seems to approach an upper limit. This is presented in figure 39, and is most likely coupled with the upper limit in $\bar{\lambda}_b$ found at high system subcooling (see figure 27). Figure 40 shows the change in the ratio of t_p and $\bar{t}_r$ as the subcooling is increased. The exponential growth in the latter figure is a natural consequence of the observed evolution in t_p and $\bar{t}_r$. However, it does not explain the observed ratio evolution. In section 3.1 we reviewed the literature in which it was explained that DWO is a result of time delayed pressure drop resulting from an earlier time flow perturbation. This pressure drop produces regenerative feedback to the boil-

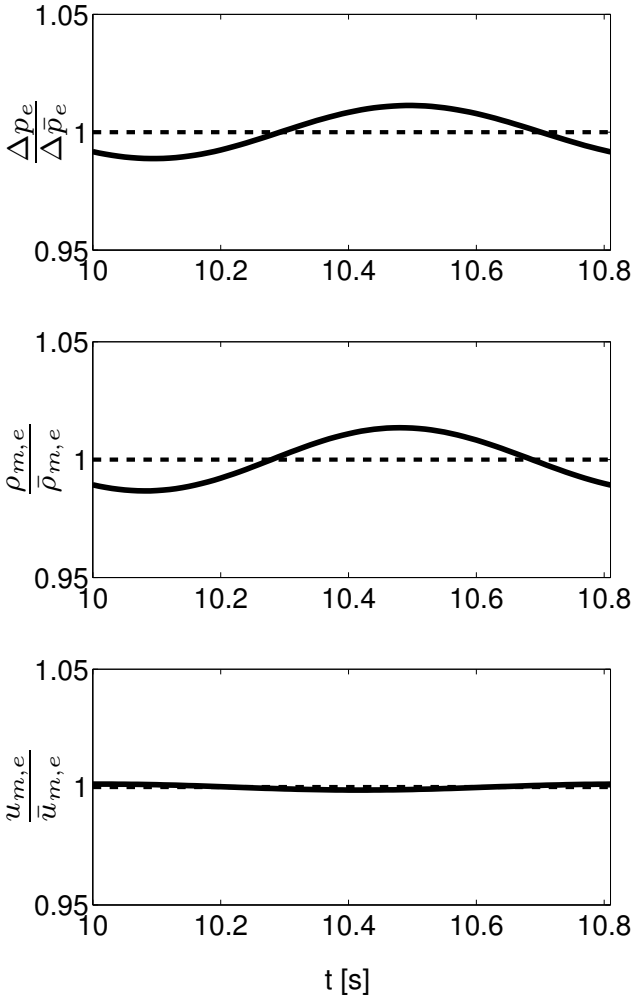

Figure 35: Oscillations in the exit restriction pressure drop Δp_e, exit mixture density $\rho_{m,e}$ and exit mixture velocity $u_{m,e}$ with respect to their mean values at *Low Subcooling*.

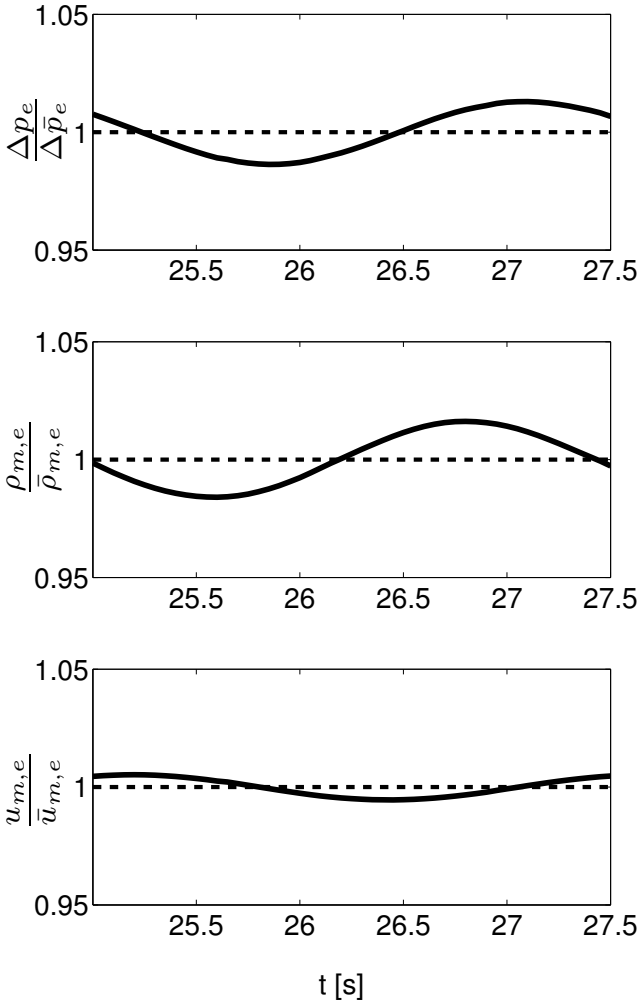

Figure 36: Oscillations in the exit restriction pressure drop Δp_e, exit mixture density $\rho_{m,e}$ and exit mixture velocity $u_{m,e}$ with respect to their mean values at *Intermediate Subcooling*.

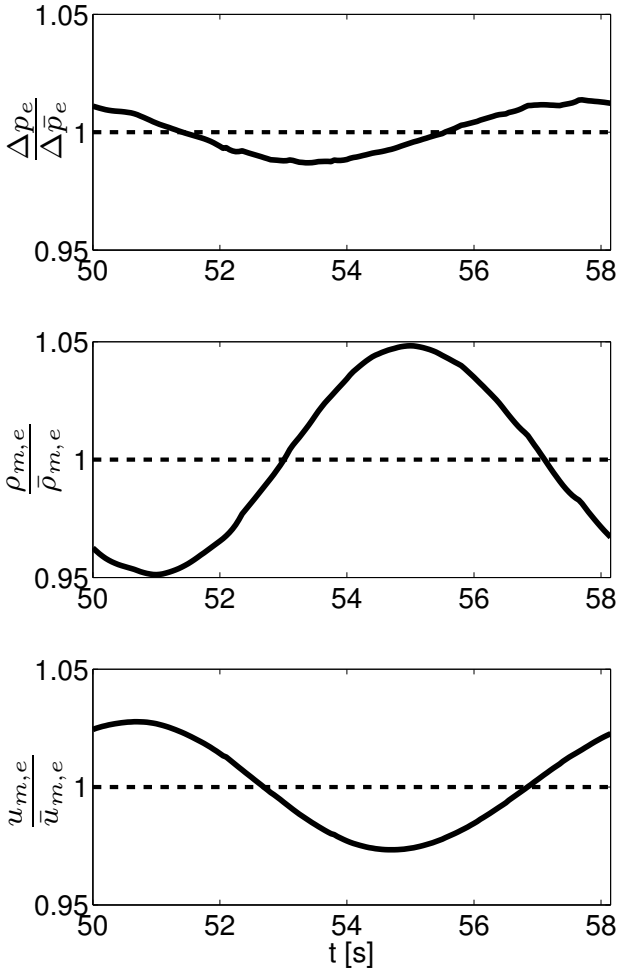

Figure 37: Oscillations in the exit restriction pressure drop Δp_e, exit mixture density $\rho_{m,e}$ and exit mixture velocity $u_{m,e}$ with respect to their mean values at *High Subcooling*.

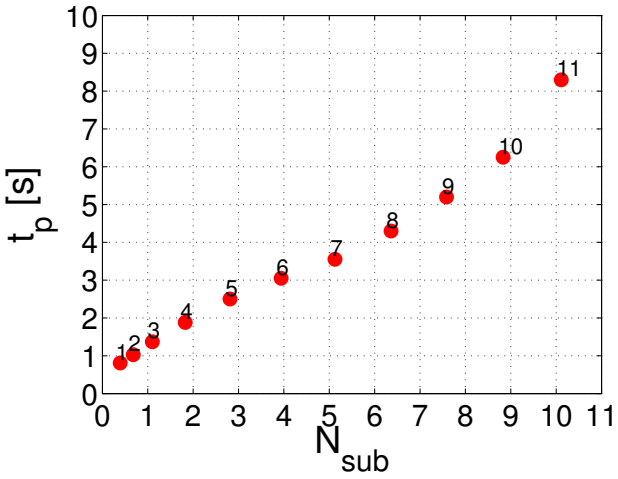

Figure 38: Evolution of oscillation period t_p for marginally stable oscillations at different levels of subcooling.

ing channel inlet, and depending on the operating condition, various oscillatory behaviors can be observed. In this thesis we have studied this downstream pressure drop by investigating the behavior of the exit restriction. The exit restriction is the most time delayed pressure drop source and consequently has the biggest destabilizing effect on the modeled system. The dynamic behavior of the system, represented by the oscillation period, is therefore thought to be a result of how the exit restriction responds to changes in exit conditions. As given by equation 40, the exit restriction pressure drop is found from the exit mixture density and the exit mixture velocity. At higher levels of system subcooling it is the exit mixture velocity that controls the exit restriction pressure drop, and the amplitude of the oscillation in exit mixture velocity increases exponentially at high subcooling. This exponential change is also seen in the oscillation period. Thus, it is concluded that it is the change towards a more velocity dominated system that causes the oscillation period to increase as it does.

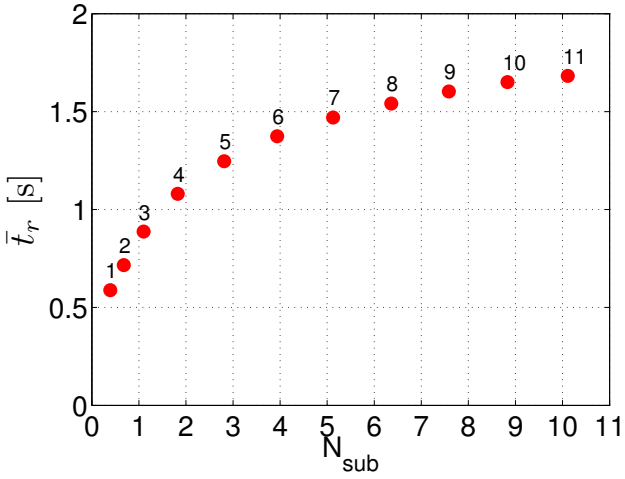

Figure 39: Evolution of mean boiling channel residence time $\bar{t}_r$ for marginally stable operating conditions at different levels of subcooling.

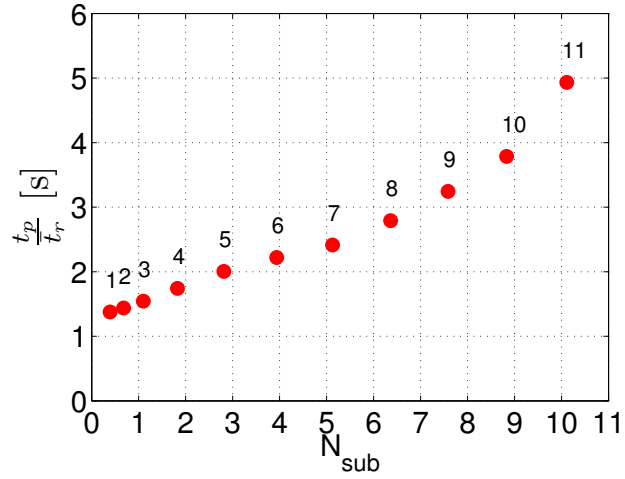

Figure 40: Evolution of the ratio between the oscillation period t_p and mean boiling channel residence time $\bar{t}_r$ for marginally stable operating conditions at different levels of subcooling.

5 Conclusion

5.1 Summary

The instability phenomena know as density wave oscillations (DWO) have been studied numerically by investigating the dynamic behavior of a horizontal single boiling channel where water at low pressure is heated with a constant uniform heat flux. Flow restrictions are placed at the inlet and exit of the boiling channel. The modeled system is subjected to a constant externally imposed pressure drop. The flow is modeled by assuming one dimensional homogenous equilibrium flow.

The work presented in this thesis is directed towards the effect of system subcooling on DWO and further how subcooling affects the governing mechanisms. The effect of subcooling is investigated by comparing modeled self-sustained periodic oscillations. Operating conditions leading to such an oscillatory behavior make up the system's stability threshold.

The flow model is validated by observing the effect of degree of subcooling on DWO characteristics and comparing the results to what has been observed in the literature. In both the classical description of DWO [Boure et al., 1973, Kakac and Bon, 2008] and Rizwan-Uddin [1994] the fundamental mechanism of DWO is found by observing how the oscillations in the exit restriction pressure drop varies with respect to oscillations in exit mixture density and velocity. The flow model is able to confirm that for a low level of subcooling it is the variation in mixture density that controls the oscillations in the exit restriction pressure drop. Hence, the exit mixture density and the exit restriction pressure drop varies almost inphase and the picture presented by the classical description is confirmed for low subcooling. At higher subcooling the modeled results show that it is in fact the variation in exit mixture velocity that controls the exit restriction pressure drop. With regards to the oscillation period and channel residence time, the model is able to show qualitatively that the ratio between the two increases with the level of applied subcooling. At the highest level of subcooling considered here it is found that the oscillation period is five times the channel residence time.

The modeled results are investigated further, and it is found that the change from a mixture density dominated exit restriction towards a mixture velocity dominated exit restriction is a smooth transition for increased degree of subcooling. As the system subcooling is increased, the amplitude of the variation in both exit mixture density and velocity grows continuously with an almost exponential growth at high subcooling. The exit restriction pressure drop is proportional to the mixture density as well as to the square of the mixture velocity, and as the amplitude in velocity variation grows, the exit mixture velocity will control the exit restriction pressure drop due to their earlier mentioned squared relationship.

The modeled stability map indicates that the stability threshold seems to approach a straight line at high subcooling. This line represents operating conditions which all have the same constant mean boiling boundary location. However, the amplitude of the boiling boundary variations about this upper mean limit grows in an exponential manner. This exponential increase is postulated to be in relation with the exponential increase seen in the amplitude of exit density and velocity

variations.

The oscillation period of the observed DWO grows continuously with larger degree of subcooling, and the period increases exponentially at high subcooling. In contrast, the mean boiling channel residence time approaches an upper mean limit at high subcooling which is most likely related to the upper mean limit found in the boiling boundary location. The ratio of the oscillation period to channel residence time consequently increases continuously with higher subcooling with an exponential increase at high subcooling. The dynamic behavior of the system, represented by the oscillation period, is controlled by how the exit restriction produces regenerative feedback to the boiling channel inlet. Since exit mixture velocity becomes gradually more dominating at higher subcooling, and the based on fact that the amplitude of variations in exit mixture velocity increases exponentially at high subcooling, it is postulated that it is the transition towards a more velocity dominated system that causes the oscillation period to evolve as it does with respect to system subcooling.

5.2 Suggestions for Future Work

The stability map and the evolution of the mean boiling boundary location presented in this work indicate that self-sustained periodic oscillations with a high degree of subcooling approach a maximum limit in the location of the mean boiling boundary. To further ensure that this is the case for our modeled system, additional simulations should be performed at higher levels of subcooling than what is the maximum level investigated here.

At higher levels of subcooling the time delay in the two-phase region is close to zero due to the dominance of mixture velocity. A change in mixture velocity is propagated instantaneously to the exit of the channel due to mass conservation. Hence, at high subcooling the time delay seen by the modeled system is only that of the single-phase region. The dynamic behavior of the modeled system with respect to the single-phase residence time and the two-phase residence time should therefore be investigated further.

References

J.-L. Achard, D.A. Drew, and R.T. Lahey. The analysis of nonlinear density-wave oscillations in boiling channels. *Journal of Fluid Mechanics*, 155:213–32, June 1985. ISSN 0022-1120.

W. Ambrosini, P. Di Marco, and J.C. Ferreri. Linear and nonlinear analysis of density-wave instability phenomena. *Heat and Technology*, 18(1):27–36, 2000. ISSN 03928764.

L.A. Belblidia and C. Bratianu. Density-wave oscillations. *Annals of Nuclear Energy*, 6(7-8):425–44, 1979. ISSN 0306-4549.

J.A. Boure, A.E. Bergles, and L.S. Tong. Review of two-phase flow instability. *Nuclear Engineering and Design*, 25(2):165–192, 1973. ISSN 00295493.

D. Butterworth and G.F. Hewitt. *Two-phase Flow And Heat Transfer*. Oxford University Press, 1979.

Bart de Maerschalck. Space-time least-squares spectral element method for unsteady flows. Master's thesis, Technische Universiteit Delft, 2003.

D.F. Delmastro, A. Clausse, and J. Converti. The influence of gravity on the stability of boiling flows. *Nuclear Engineering and Design*, 127(1):129–39, May 1991. ISSN 0029-5493.

Y. Ding, S. Kakac, and X.J. Chen. Dynamic instabilities of boiling two-phase flow in a single horizontal channel. *Experimental Thermal and Fluid Science*, 11(4): 327–342, 1995. ISSN 08941777.

T. Dogan, S. Kakac, and T.N. Veziroglu. Analysis of forced-convection boiling flow instabilities in a single-channel upflow system. *International Journal of Heat and Fluid Flow*, 4(3):145–156, 1983. ISSN 0142727X.

G. Guido, J. Converti, and A. Clausse. Density-wave oscillations in parallel channels-an analytical approach. *Nuclear Engineering and Design*, 125(2):121–36, February 1991. ISSN 0029-5493.

M. Ishii. *Thermally Induced Flow Instabilities in Two- Phase Mixtures in Thermal Equilibrium*. PhD thesis, School of Mechanical Engineering, Georgia Institute of Technology, Atlanta, June 1971.

M. Ishii and N. Zuber. Thermally induced flow instabilities in two phase mixtures. *Proceedings of the fourth international heat transfer conference*, B5.11, 1970.

S. Kakac and B. Bon. A review of two-phase flow dynamic instabilities in tube boiling systems. *International Journal of Heat and Mass Transfer*, 51(3-4):399–433, February 2008. ISSN 0017-9310.

Sadik Kakac and Liping Cao. Analysis of convective two-phase flow instabilities in vertical and horizontal in-tube boiling systems. *International Journal of Heat and Mass Transfer*, 52(17-18):3984–3993, 2009. ISSN 00179310.

J. March-Leuba. Density-wave instabilities in boiling water reactors. Technical report, Oak Ridge National Laboratory, 1992. Prepared for U.S Regulatory Commision.

J. March-Leuba and J.M. Rey. Coupled thermohydraulic-neutronic instabilities in boiling water nuclear reactors: A review of the state of the art. In *Nucl. Eng. Des. (Netherlands)*, volume 145, pages 97–111, Netherlands, November 1993.

H. Muller-Steinhagen and K. Heck. A simple friction pressure drop correlation for two-phase flow in pipes. *Chemical Engineering and Processing*, 20(6):297–308, November 1986. ISSN 0255-2701.

Svend Tollak Munkejord. *Analysis Of The Two-fluid Model And The Drift-flux Model For Numerical Calculation Of Two-phase Flow*. PhD thesis, Norwegian University Of Science And Technology, 2006.

Jesus Moreno Quiben. *Experimental And Analytical Study Of Two-phase Pressure Drops During Evaporation In Horizontal Tubes*. PhD thesis, Swiss Federal Institute of Technology Lausanne (EPFL), 2005.

Rizwan-Uddin. On density-wave oscillations in two-phase flows. *International Journal of Multiphase Flow*, 20(4):721–737, 1994. ISSN 03019322.

Rizwan-Uddin and J.J. Dorning. Some nonlinear dynamics of a heated channel. *Nuclear Engineering and Design*, 93(1):1–14, 1986. ISSN 0029-5493.

L. Ruspini, C. Dorao, and M. Fernandino. Simulation of a natural circulation loop using a least squares hp-adaptive solver. *Accepted to Mathematics and Computers in Simulation.*, 2009.

L.C. Ruspini, C.A. Dorao, and M. Fernandino. Dynamic simulation of ledinegg instability. 2(5):211–216, 2010. ISSN 18755100.

P. Saha and N. Zuber. An analytical study of the thermally induced two-phase flow instabilities including the effect of thermal non-equilibrium. *International Journal of Heat and Mass Transfer*, 21(4):415–26, April 1978. ISSN 0017-9310.

P. Saha, M. Ishii, and N. Zuber. Experimental investigation of the thermally induced flow oscillations in two-phase systems. *Journal of Heat Transfer*, 98 Ser C(4):616–622, 1976. ISSN 00221481.

X.-H. Sun, Z.-H. He, Z.-C. Huang, W.-J. Xiao, X.-M. Qi, A. Pauw, and J. van Es. Analysis of temperature oscillations in parallel evaporators of a carbon dioxide two-phase loop. *Microgravity Science and Technology*, 21:S299–S304–, August 2009. ISSN 0938-0108.

Graham B. Wallis. *One-dimensional Two-phase Flow*. McGraw-Hill Book Company, 1969.

Frank M. White. *Viscous Fluid Flow*. McGraw-Hill Book Company, 1991.

H. Yuncu, O.T. Yildirim, and S. Kakac. Two-phase flow instabilities in a horizontal single boiling channel. *Applied Scientific Research*, 48(1):83–104, January 1991. ISSN 0003-6994.